UNITED STATES DEPARTMENT OF THE INTERIOR
GEOLOGICAL SURVEY

Geologic Factors Affecting Seismic Monitoring in China

John R. Matzko[1]

Open-File Report 95-562

[1]Reston, Virgina

1995

Geologic Factors Affecting Seismic Monitoring in China

Table of Contents

List of Figures

List of Tables

Introduction

The purpose of this report is to provide a basic geologic and environmental background to researchers, in support of nuclear test detection in China under a Comprehensive Test Ban Treaty (CTBT). One of the main concerns of a CTBT is the ability of an international monitoring system to detect covert nuclear testing. Evasion scenarios typically consider the potential for hiding tests in geologic media favorable for full or partial decoupling, or in an area of natural or man-made (i.e., mining) seismicity. The environments considered in this report, which may have potential for decoupling, include natural or man-made cavities (such as natural caverns or mined cavites in hard rocks, karst caves in limestones, or mined salt cavities), or thick sequences of dry, unconsolidated material, such as sand or loess. The report also gives a basic introduction to the nature of the Earth's crust in China. Sections in the report describe the natural seismicity, locations and types of neotectonic activities, recent volcanism, crustal thickness and characteristics, and heat flow, all of which may influence either the coupling of seismic energy to the rocks or the propagation of the seismic wave through the crust to the seismic detectors. Knowledge of the geology is also useful for characterizing and evaluating current or potential nuclear test sites for explosion yield deteminations and for containment.

China is located on the southeastern edge of the Eurasian continent, between about 72^0 to 135^0 east longitude, and about 20^0 to 52^0 north latitude. With a total land area of 9,326,410 km^2, China is slightly larger in area than the contiguous United States (CIA, 1979; 1989, p. 61). Such an expansive country is characterized by a wide diversity in such features as weather and climate (tropical in the south, subarctic in the north), topography (mountains, high plateaus and deserts in the west; plains, deltas and hills in the east), vegetation, groundwater characteristics, rock environments, and geologic structure. Most of the precipitation, agriculture, population and industry are concentrated in the eastern half of China, while most of western China is desert with less than 400 mm annual precipitation. The country has abundant natural resources and is the world's leading producer of coal. China is also ranked among the top four world producers of salt, manganese and iron ores, crude petroleum, phosphate rock, tin, zinc, and rare earth elements. China also has the world's largest hydropower potential (CIA, 1989; U.S. Dept. of Interior, 1993).

One of the earliest western works concerned with establishing a country-wide geologic and tectonic framework in China is the 5-volume, multiple-authored *Atlas of Asia and Eastern Europe to Support Detection of Underground Nuclear Testing*, published by the Dept. of Interior, U.S. Geological Survey, for ARPA, between 1966 and 1969 (see Lang and Sun, 1966, in the References). Volume II (*Teconics*) of this atlas contains an important tectonic map of China and Mongolia, which has been separately published by the Geological Society of America as the *Tectonic Map of China and Mongolia*, by Maurice J. Terman, principal compiler (see Terman and others, 1974, in the References).

Rock Environments

China contains a diverse range of geologic environments, including all major lithtologic groups. The simplified geologic map in Figure 1 presents the distribution of the main rock types in China.

Igneous Rocks - *Granites and Basalts*

Granitic and related rocks are widespread throughout all regions of China, and account for about one third of the total exposed area of bedrock in the country . They often form the majority of rock in some mountain ranges (United Nations, 1986). In Northeast China (Manchuria), they occur in two NE-trending belts, forming much of the Greater and Lesser Khingan Ranges on the northwest side of the region, and the Heilongjiang mountain system on the southeast side.

Extensive occurrences of basalt, including dense and vesicular varieties, are found in the same areas (see the section below on Quaternary Volcanism).

In the North China region (the area of the Bo Hai Sea and further west), granitic and basaltic rocks generally form some mountains and hills along the northern margin (Gobi Desert - Yin Shan mountains) and southern margin of the area (Tsinling Shan mountains), but are most widespread in the eastern part and on the Shantung Peninsula, which separates the Bo Hai and Yellow Seas.

In South China, the granitic rocks are most common along the southeast coast (Wu-i-Shan and Nan Ling Mountains of the Cathaysian fold system; also see Figure 3). There are smaller occurrences in the extreme western part of the region, near the border with Burma, and along the northern margin of the region, most notably in the Ta-Pieh mountains. Basaltic rocks are not as widespread, and are restricted to the northern part of Hainan Island and small exposures on the adjacent peninsula, and to a north-south trending belt between about 102^0 and 105^0 east longitude in the Yunnan area. Small occurrences are also found in the eastern margin of the region, to the northwest and south of Shanghai.

In the Xinjiang region, granitic rocks are confined to the east-west trending mountains (Altai, Tien Shan, Kunlun Shan mountains) that bound the two main basins in the region (Tarim and Junggar basins). Basalts are not as common and are found only in a relatively thin east-west trending belt in the Tien Shan Mountains, and in very limited areas near the extreme western rim of the Tarim basin and as small occurrences on the northwestern and southeastern margins of the Junggar basin.

Granitic rocks are most commonly found in the eastern half of the Tibet highland region, in NW-SE trending belts. There are smaller, sporadic occurrences along the southern and western borders, in the Himalayas. Areas of basaltic rocks are very limited, and are found mostly in a small area in the extreme southeastern corner of the region and near the western border with India, but are also found in isolated areas in the Himalayas.

Metamorphic and Sedimentary Rocks

As seen on the map of the distribution of carbonate rocks in China (see Figure 20, below, in the section on Karst), limestones are wide spread throughout China, but are most common in the southwestern and southern regions. In Northeast China (Manchuria), limestones, sandstones, shales, and tuff are distributed in small areas near the southern margin of the Jehol mountains at the southern end of the Greater Khingan Range, and also in the Heilongjiang mountains. The sandstones, shales, and tuff are also common in the Lesser Khingan range and the northern end of the Greater Khingan Range. Schist, interbedded with quartzite, slate, and marble, is found in the area of the Heilongjiang mountains, and in more limited areas of the Greater Khingan Range.

In North China, limestones are most common in the eastern part of the region, in the Central China Uplands. Shale, sandstone, conglomerate, and schist occur in the same general areas as the limestones, which are locally interbedded with shales and sandstones. The limestones are cavernous, jointed and fractured. The sandstone and conglomerate are interbedded with shale and limestone, and are locally associated with tuffaceous rocks, gypsum, and coal. Limestone, sandstone, shale, conglomerate and schist also occur in the Pei-Shan and Nan Shan mountains in the extreme west, and in the Tsinling Shan mountains on the southwest margin of the region. Sandstone and conglomerate, with lesser amounts of shale, slate, and schist, are found in the area of the Gobi Desert, at the northern margin of this region.

Slate, schist, and shale are dispersed throughout South China. They comprise the dominant rock types in the central and western portions of the region, but are also common in the eastern portion. Associated subordinate rock types are marble, quartzite, limestone, sandstone, and coal.

Sandstone and conglomerate, interbedded with subordinate amounts of shale, limestone, and coal, occur in the mountains, hills, and intermontane basins of the Southern Uplands (Cathaysian fold system and southern parts of the South China platform - see Figure 3) and Central China mountains (northeastern part of the South China platform; and south central part of the Central China fold system, as defined in Figure 3). Limestones are most widely distributed in the central areas of South China, with lesser occurrences in the northwest and west. The Yunnan and Guizhou plateaux, and the Guangxi plains of South China are carbonate regions famed for the development of spectacular tower karst (see Figure 21, below) in carbonate sequences which are thousands of meters thick.

In Xinjiang, slate, schist, shale and limestone are common in the Tien Shan and Kunlun Shan mountains; the limestones become less abundant in the latter. The slate and schist are associated with lesser amounts of marble, quartzite, and shale, with some limestone, sandstone, and coal beds. Some limestone is found in less extensive areas on the eastern and western margins of the Junggar basin. The limestone is locally interbedded with shale, sandstone, and tuffaceous rocks. Sandstone and conglomerate occur in lesser amounts in the Tien Shan and Kunlun Shan mountains, but become the dominant rock type in the hills and plains south of the Altai mountains, on the northern margin of the Junggar basin. The sandstones and conglomerates are interbedded with shale, limestone, tuff, and coal.

The vast majority of the area of Tibet is composed of slate, schist, and shale. Limestone is found in three belts that trend generally east-west. The smallest belt borders the Qaidam basin on the north. The largest belt extends from the western margins of the region to the southeastern, forming part of the Kunlun Shan mountains and smaller ranges. The southernmost belt also extends east-west across the length of the region, forming the Trans-Himalaya mountains. The limestones are jointed, fractured and cavernous in places. They are locally interbedded with shale, sandstone, and volcanic rocks. The occurrences of sandstone and conglomerate are few, and limited mostly to a relatively small area in the eastern part of the region. There are also a few small occurrences on the margins of the Qaidam basin, and in areas along the southern border.

Ground Water Occurrences and Conditions

In general, most of northeastern, eastern, and southern China receive precipitation in excess of 400 mm - see Figure 2. These regions are most likely characterized by the occurrence of shallow ground water tables, which probably occur at depths of less than 50 m throughout these regions. In those areas where thicker accumulations of soil and unconsolidated overburden exist, the shallow groundwater table is likely to be unconfined. Deep water tables (in excess of 50 m depth) are most likely to be found in the arid areas of China, which are limited to the northwestern parts of the country, as shown by the precipitation map in Figure 2. Because of the lack of cultural activity in these arid regions, there are few data detailing the depth to ground water here. However, some comments on ground water and the potential for occurrence of thick, dry, unconsolidated sediments in some areas can be made based on the limited information available.

Much of northwestern China is characterized by mean annual precipitation rates of 200 mm or less, with significant desert areas receiving 100 mm or less annual precipitation. The mean annual evaporation rates of 1500 mm greatly exceed the precipitation rates (Jiao Shuqin, 1985; United Nations, 1986, p. 84). However, abundant precipitation and snowfall in the adjacent mountains provide some ground water recharge to the basins.

The greatest potential for the occurrence of thick, dry unconsolidated material is found in the western interior desert basins of China. The mountains encircling the basins are flanked by broad, sloping piedmont plains composed of significant thicknesses of unconsolidated gravel, sand, and sandy clay. Occasionally, the subsurface of the piedmont plains is interrupted by uplift structures which interfere with the subsurface migration of groundwater. For example, uplift structures

occur on the southwestern edge of the Tarim basin (the piedmont belt on the north flank of the Kunlun Mountains). On the south side of the buried uplifts, ground water is found at depths of about 30 m, but is deeper on the north side of the structures. The depth to ground water is also greater than 30 m on the south eastern edge of the Tarim basin, in unconsolidated sediments several hundred meters thick (Jiao Shuqin, 1985). In the piedmont belt on the north flank of the Tien Shan mountains (southern margin of the Junggar basin), ground water is found at depths generally greater than 50 m (United Nations, 1986, p. 84). The desert interiors are generally covered by sand dunes, which commonly range in height from less than 5 m to 10 - 25 m; some are 100 - 300 m high. With the exception of the dunes in the Takla-Makan desert of the Tarim basin, the dunes can often contain small lenses of unconfined water generally at 1 - 10 m depth, becoming deeper with increasing height of the dune. Ground water can also occur as pore water in the Quaternary sediments underlying the dunes. The maximum thickness of the Quaternary sediments in the Tarim and Junggar basins is about 1 km (Terman and others, 1974).

An unconsolidated sequence with a thickness to 200 m or greater occurs in limited areas of the loess plateau (southern end of the Ordos desert), but the precipitation rates are greater here, up to 500 mm. The maps in Figures 21 and 22 in the section below on Loess, shows the thickness distribution of these sediments. Additional detail on the potential depth to ground water in this material is given in the section on Loess.

Principal Tectonic Regions

The basic tectonic framework of China is described briefly in this section. The current and recent tectonic activity in the country is described below, in the sections on Active Tectonics and Quaternary Volcanism.

The locations of major platforms and fold systems which comprise the main tectonic elements of China are given in Figure 3, which is modified from Terman and others, 1974. The figure also shows the locations of some of the basins and mountain ranges discussed in the text. The present landmass of China has evolved through the accretion of island arc systems and relatively small continental blocks onto the Siberian craton, which lies to the north (Ma Xingyuan, 1986, p. 5). These accretionary processes apparently continued untill the collision of the Indian plate with Asia in early Tertiary times. The Tarim, Sino-Korean (also called North China platform by some researchers), and the South China (Yangzi) are three major Precambrian platforms which form the backbone of mainland China. These platforms represent ancient stable continental blocks around which the various fold belts were formed and consolidated by different tectonic cycles in the Precambrian through Cenozoic eras. The process of accretion and growth of the Sino-Korean platform ended with its consolidation about 1.8 billion years ago, making this platform the geologically oldest region in China. The Tarim and South China (Yangzi) platforms are younger, being consolidated about 700 to 850 million years ago, towards the end of the Precambrian era (Meyerhoff and others, 1991, p. 116).

The tectonics of western China (west of the Helan-Liupan-Longmen line; see the crustal thickness map in Figure 7, below) are characterized by east-west structural trends, north-south oriented compression, the rejuvenation of east-west trending fold belts, several intermontane basins (stable blocks), and significant strike-slip and thrust faulting. Predominant fracture directions are NW, WNW, and ENE. Eastern China is characterized by strike-slip and normal faults which change their orientation to NE - NNE. Eastern China also contains a broad zone of compressional and tensile horst and graben structures, continental volcanism, and major intrusions of igneous rocks that trend NE and NNE. There are also compressional island-arcs and related systems along and east of the southern continental margin. The predominant trends of fractures in eastern China are NE, NNE and NNW (Meyerhoff and others, 1991, p. 129, 134).

Major fault zones throughout the country are commonly 25 to 40 km wide (Meyerhoff and others, 1991, p. 119, 134). On the basis of depth plots of earthquake foci, Das and Filson (1975) find no evidence of any major subduction zone in the interior of eastern Asia. Instead, they find that shallow seismicity is indicated in the Hindu Kush-Lake Baikal and Himalaya-Tibet regions. Subduction of the northeast flank of the Indian plate beneath Burma is suggested by deep earthquake foci (to about 200 km depth) on an east-dipping slab.

Active Tectonics

The continental area of China is very tectonically active. Earthquakes occur on most of its territory; active faults are found throughout the country; significant uplift has occurred in the west; there are many areas of subsidence in the east with the formation of grabens and rifts; and abundant volcanism occurs in the east and south. Although seismic events are widespread throughout the country, China is considered to have only moderate levels of seismicity. For example, the number of shallow earthquakes (less than or equal to 40 km depth) with m_b greater than or equal to 5.0, over the ten year period from 1981 to 1990, is 215 in China versus 171 in the contiguous United States. (If Alaska and Hawaii are included in the U.S. numbers, that figure then jumps to 606 events).

Neotectonic movement in continental China is influenced by three main factors. The greatest influence is exerted by the convergence of the Indian plate with Eurasia which, in the Tibet area, began about 40 - 50 million years ago (early Tertiary). The Indian plate is continuing its northward motion at a rate of about 4 - 5 cm/year (Ma Xingyuan, 1986, p. 7) and has resulted in the rejuvenation of tectonic activity in the mountains and compressional basins in the northwest. The second factor is the subduction of the Pacific plate along the Japan trench, which has resulted in back-arc spreading and uplift of the mantle in North China (in the area of the Bo Hai Sea and further west). The mantle uplift has caused crustal thinning and stretching in this area, developing basin and range structures (rift grabens) with a NNE trend. The third factor, which exerts the least influence on neotectonic activity in China, is the subduction of the Philippine Sea plate along the Ryukyu-Taiwan-Luzon trench; the motion vector of this subduction is directed to the northwest such that it apparently influences only Taiwan and the southeast coastal area of the Chinese mainland. Complex intraplate fracturing patterns and strong seismicity are features of neotectonic activity throughout China. The major active fault belts in China and some associated focal mechanism solutions are given on the map in Figure 4.

Uplift of the Qinghai-Tibet (Xizang) plateau has been rapid, with as much as 3700 m of uplift during the Quaternary Period (Cao Jiadong and Shao Shixiong, 1991). The present altitude of the plateau is 4500 to 5000 m above sea level. In the Tien Shan mountains uplift during the late Neogene through Quaternary was about 2500 m (Ma Xingyuan, 1986). The continental collision produces north-south compression in western China, generating neotectonic features with generally east-west orientations. Western China is thus characterized by several east-west trending folded and faulted mountain ranges (Altai, Tien Shan, Altun Shan, Kunlun Shan) which are apparently reacting to the continental collision, while intervening compressional basins (Junggar, Tarim, Turpan, Qaidam basins) act as stable blocks and remain relatively undeformed, apparently transmitting the stress to the fold belts on the periphery of the blocks. Late Neogene to Quaternary subsidence has been as much as 5,000 m in the Junggar basin; 1,000 m in the northwestern and western parts of the Tarim basin, and up to 2500 m in the Qaidam basin (Ma Xingyuan, 1986). Although many relatively smaller earthquakes are known to occur within the stable blocks, most major earthquakes occur on the basin margins, in or near the fold belts. Most of the major faults occur within the foldbelts and consequently also follow a general east-west trend, but NE, NW and NNW trending faults are also common. The faults that more nearly parallel the east-west trending North and South Tien Shan mountain ranges are mainly reverse, thrust, or overthrust faults, while strike-slip movement is common on faults trending more obliquely. Fault plane solutions,

geologic data, and in-situ stress measurements in mines in western China suggest that the principal compressive stress is nearly horizontal and trends north-south to northeast-southwest, approximately perpendicular to the strikes of the rejuvenated Mesozoic and Paleozoic fold belts (Molnar and others, 1973, p. 106-108). Although many fault solutions here indicate thrust faulting, large strike-slip faults, some showing left-lateral displacement, also occur within and along the fold belts, and probably accommodated some of the relative motion between the Indian and Eurasian plates (York and others, 1976, p. 1993).

The tectonics of eastern China differ significantly from those of western China in that seismic activity in the east is not concentrated in fold belts. Stable blocks in the east include the South China, Ala Shan, Ordos, and Shansi blocks, which are separated from each other by zones of block faulting, rifting, or volcanism, rather than fold or thrust zones. Fault plane solutions determined from many earthquakes in eastern and northeastern China indicate predominantly strike-slip faulting; the sense of displacement is commonly right-lateral. Normal faulting also occurs. Another significant difference in the tectonics between western and eastern China is the northeastern trend of mountain ranges in the eastern half of China, compared to the east-west trending mountains in the west. The average elevations in western China are also higher than the average elevations in eastern China.

Neotectonic activity in Northeast China is affected by the subduction of the Pacific plate in the Japan trench. The main features of this area are the strong volcanic activity and the deep focus seismicity. In this region, faults are generally of a smaller scale and less active than those seen in the west, and trend mostly NE and NW. Differential uplift and subsidence in this region is not great. Maximum subsidence in the Songliao region (which includes the Songliao plain and the Lower Liaohe River plain, on the northeast side of Bo Hai Sea) has been only 200 to 400 m during the Quaternary (Cao Jiadong and Shao Shixiong, 1991, p. 29). Further north, subsidence in the Songliao basin is indicated by Ma Xingyuan (1986) to be up to 100 m. Subsidence in the area of the North China Plain (west of Bo Hai Sea) is as much as 500 m. Rift basins (grabens) such as the Songliao basin, and intervening ranges trend to the NE.

North China includes the region of the Bo Hai Sea and areas further west. This region is located at the junction of several tectonic plates and consequently displays some of the strongest tectonic movement in China, in the form of intense differential vertical movement, relatively strong seismicity, and development of rift basins. Faults are mostly left-lateral strike-slip and normal, with dominant trends of NE and NNE. In the North China area, the tensile strain is greater than the compressive strain (Cao Jiadong and Shao Shixiong, 1991, p. 40). Maximum subsidence in the area of the Bo Hai Sea - North China plain during the Quaternary is greater than 650 m. The estimated average subsidence rate of the Hebei Plain (northern part of the North China plain) during the Quaternary is 15.4 cm per thousand years. Locally, subsidence has been intermittent, with even local uplift occurring (Shao Shihxiong and others, 1982, p. 5-7). The vertical movement has caused fracturing, which has localized the centers of volcanic eruptions. As shown on the map in Figure 5, volcanic activity is common on the North China plain. The plain itself is a graben (rift basin), which was initiated in early Tertiary time. The subsidence and rifting in this region correspond to an area of mantle uplift (see the crustal thickness map in Figure 7, below), which explains the thin crust, high heat flow, and common volcanism, characteristic for this area.

South China is a relatively stable area where differential movement is not as pronounced as in North China. Seismicity is generally weaker in South China, except along the southeastern coastal areas. The entire region is undergoing slow uplift due to NW-SE directed compressive stresses apparently resulting from the subduction of the Philippine Sea plate to the southeast. Several NW-trending extensional basins have developed in this region. Hydrothermal, multiphase volcanic activity, and seismic activity characterize the neotectonic features of the eastern part of the region.

Very strong neotectonic activity occurs in the Taiwan-East China Sea area, which is influenced by the subduction of the Philippine Sea plate. Taiwan is part of the Ryukyu-Taiwan-Luzon island arc system which is currently active. Strong orogenic movement has produced tight linear folds, reverse faults and regional metamorphism on Taiwan. The subduction of the oceanic plate has caused strong volcanism on and near the island, most notably the Datun and Jilong volcano groups. The plate subduction directs NNW-SSE trending compression on the island, resulting in mainly horizontal stresses. Plate convergence is presently about 7 cm/year. Taiwan is undergoing strong vertical movement with rapid elevation of the crust (mean elevation rate is estimated at about 5 mm/year). Significant neotectonic activity here includes crustal uplift, faulting and block activity, folding, eruption of mud volcanoes, development of hot springs, and frequent seismicity - over half of the earthquakes recorded in China in the past century were located on Taiwan (see the section below on Seismicity) (Cao Jiadong and Shao Shixiong, 1991)

The area of southern China, near Burma, is complicated by the interaction of the northward-moving Indian shield and the resistant Eurasian continent. This area is characterized by regions with relatively high levels of seismicity, which include normal, strike slip, and thrust faulting, and indicate a region with a complicated pattern of deformation (Molnar and others, 1973, p. 107). Fault plane solutions and topographic evidence indicate that displacement along the fault zone at about 100^0 E longitude, between Burma and the Sichuan basin, is left lateral. This would suggest that this area is either moving independently of the India-Eurasia collision, or it is being squeezed out of the area by the collision (York and others, 1976, p. 1998)

Maximum and minimum compressional principal stress axes are horizontal for most areas of China, although the maximum compressional principal stress axes are vertical for some areas where both normal and strike-slip faults are common (some areas of North China; the southern section of the Fen-Wei graben; northern Jiangsu and NW Liaoning). The map of the recent tectonic stress field of China in Figure 5 shows the distribution of the maximum (compressional) and minimum (tensile) principal stress axes throughout the country. This distribution suggests that the stress, manifested by tectonic activity and seismicity, is not produced by internal or local causes, but rather is related to the plate motions acting along the periphery of China (Cao Jiadong and Shao Shixiong, 1991, p. 39). The map in Figure 5 indicates that in western China, the maximum compressional principal stress axis trends about N-NE to S-SW, with the secondary tensile stress axis roughly perpendicular to this direction. Further to the east, the maximum compressional principal stress axes bend around the northeast corner of the Indian plate in the area of Burma (where the eastern part of the Indian plate is being subducted), such that the stress trajectories fan out eastward and change their orientation to NE-SW over North and Northeastern China; and eventually obtain a NW-SE orientation in South China and Taiwan.

Quaternary Volcanism

The distribution of Quaternary volcanoes in China and the time sequence of their activity is controlled by neotectonic movement in the country. Over 700 Quaternary volcanoes are known in China, though fissure eruptions (from calderas) were apparently more common in the Neogene and early Quaternary. The Quaternary rocks occur both as cones and lava plateaus. More than 80% of the Quaternary volcanoes in China are located in the eastern half of the country: in Northeast China, North China, Southeast China, South China Sea, and Southwest China. The only volcanoes in western China are the Middle and Late Quaternary volcanics located near the southern margin of the Tarim Basin, in the region of the Altun-Tagh major left-lateral strike slip fault. The distribution of volcanoes in China is given on the map in Figure 6.

In China, there are five major volcanic belts, or regions, which parallel fracture zones (see Figure 6). In eastern China, the subduction of the Pacific plate beneath Eurasia has resulted in updoming of the mantle and thinning and stretching of the crust in the region of the Bo Hai Sea. A

series of NE to NNE trending fractures and down-faulted basins formed, which were intruded by magmas to form the eastern Chinese volcanic belt of the Circum-Pacific volcanic belt. Here, Quaternary volcanoes are located in three NE to NNE trending belts: the Khingan Mountains - Taihang Mountains volcanic group; the Changbai Mountains - Longgang Mountains volcanic group; and the Southeastern Coastal belt. Uplift continues on the Qinghai-Tibet plateau in western China. An east-west trending volcanic belt is located on the northern margin of the plateau; this belt is composed of Tertiary and Quaternary-aged rocks, mostly in the West Kunlun area of northern Tibet. In southern China, the north-south trending Western Yunnan volcanic belt is located on the south-eastern tip of the Tibet plateau, in the region where the northeastern edge of the Indian plate is being subducted beneath Burma.

The extent of volcanic outpourings varies from a few dozen square kilometers in area and less than 40 m thick (Taihang Mountains volcanic group), to over 9200 square kilometers in area with thickness to 70 - 280 m. (Abag - Huilong volcanic group of the Khingan Mountain - Taihang Mountains volcanic belt). The lavas of the Western Kunlun - Hoh Xil volcanic belt of northern Tibet cover an area of 1088 square kilometers and are up to 300 m thick. In eastern China, rocks of basic composition (basalt, basanite) are the most common among the Quaternary volcanics, and occasionally contain inclusions of mantle-derived rocks (peridotite, dunite). In western and southwestern China, the Quaternary volcanic rocks are generally of more intermediate chemical composition (andesite and dacite) (Zhang Yufang, 1991).

Several volcanoes have been active in historical times. The most recent volcanic event was the May 27, 1951 eruption of the No. 1 volcano of the Kardaxi Group, in the Western Kunlun volcanic belt of northern Tibet. Several historic eruptions of Mt. Baitou (in the Changbai Mountains volcanic group of northeastern China) were almost synchronous with eruptions in Japan, suggesting to Zhang Yufang (1991, p. 285) that there may be an internal connection between the two regions. Volcanic activity also continues on Taiwan. Hot springs and fumaroles are known in the Datun area where the hot water from drill holes can reach 295^0 C. Clusters of active mud volcanoes are also known from southern Taiwan and the Coastal Mountains in the east (Zhang Yufang, 1991, p. 305).

Crustal Thickness and Characteristics

The continental area of China has one of the most complex lithospheric structures in the world, with crustal thickness ranging from less than 30 km in eastern China, to 70 to 80 km under the Qinghai-Tibet plateau in the western regions, which is about twice the thickness of normal continental crust (Huang and Wang, 1991b). The thickness of the crust in China is given on the map in Figure 7. This map clearly shows major differences in the crustal thickness between western and eastern China, as defined by the roughly north - south trending Helan - Liupan - Longmen line, which is annotated on the map. This line, and the Khingan - Taihang - Wuling line further to the east, mark the locations of abrupt changes in depth to the Mohorovicic discontinuity (Meyerhoff and others, 1991, p. 129). The Tibet block is encircled by narrowly-spaced depth contour lines, forming steep "slopes" down to the base of the crust. The eastern edge of the plateau is characterized by a deep-seated earthquake belt and an imbricated mountain belt, in the area of the Helan-Liupan-Longmen line. Zhang and others (1984, p. 310-311) suggest that this, along with the abrupt change in crustal thickness, indicates that the Qinghai-Tibet plateau is decoupled from eastern China along this north-south boundary. The depth contours in western China generally display an east-west trend, reflecting the trend of structural features seen on the surface. In contrast, the crust of eastern China is much thinner, ranging from less than 30 to about 45 km thick, which is a more normal thickness expected for continental crust. The trend of the contour lines also changes to north-northeast to south-southwest, highlighting the difference in the geologic history and tectonics of the two regions. The differences in the crust may be due, at least in part, to the collision of India with the Eurasian continent, which is subjecting western China to

compressional tectonics, while eastern China appears to have been subjected to tensile conditions during the Mesozoic and Cenozoic, as indicated by the formation of grabens and locally thinned crust (Zhang and others, 1984).

Over the past 40 years, China has conducted a Deep Seismic Sounding (DSS) program to investigate the properties of the crust in several regions of the country (Huang and Wang, 1991b), though few data regarding this program have been found to date. Unlike the Russian DSS program, the Chinese have apparently not used nuclear explosions as seismic sources. The locations of the DSS lines (see Figure 8) suggest that this work has been more extensive in the more highly populated areas of North and South China, while few, if any, investigations are noted in northeast and northwest China. Based on these investigations, average Pn velocities and crustal thickness for regions encompassed by boxes on the map, are tabulated in Table 1. Additionally, section I of Figure 9 presents six P-wave velocity models of the crust and upper mantle for certain areas of China. These profiles show an upper mantle low-velocity zone (LVZ) between 100 to 150 km depth, for each of the seven regions depicted, with the exception of the South China profile. Section II of Figure 9 presents an additional ten velocity models limited to characterizing the crust in some parts of China. These ten profiles clearly show the differences in crustal thicknesses between eastern and western China as exemplified by profiles K (southern part of Liaoning Province, northeast China; crust is about 28 km thick) and O (north part of the Himalayas; crust is about 75 km thick). Several profiles (I, J, K, M, N, an P) show apparent shallow crustal low-velocity zones. There is also some evidence for a 10 km thick low velocity zone between 20-30 km depth under the Qinghai-Xizang plateau (Meyerhoff and others, 1991, p. 146). Additionally, Revenaugh and Sipkin (1994) indicate mid-lithospheric LVZs occur under the Tibetan Plateau and the fold belts to the north. They also state that there is no seismic evidence for the presence of similar LVZs under Mongolia, southeastern Russian, and northeastern China.

Seismic body wave propagation across the Chinese mainland may be attenuated or otherwise influenced by the thick accumulations of sedimentary deposits in many of the large oil-producing basins of the country, which are shown in Figure 16. Because the structure of the western basins is different from those in the east, the locations of the thickest sedimentary deposits within the basins is also different. The following descriptions of the basins are taken from Meyerhoff (1982).

The western basins are characteristically ringed by marginal foredeeps, in which the thickest sedimentary accumulations are found. The central parts of these basins are occupied by median massifs, in which the basement arches up nearer to the surface, such that the sedimentary cover here is a fraction of the thickness of the sediments in the foredeeps. For example, the Junggar and Tarim basins contain up to 11 km of Mesozoic and Cenozoic sediments in certain marginal troughs, but these sediments thin over the central basin uplifts so that they are only about 3.5 km thick in the Junggar basin, and less than 1 km thick in the middle of the Tarim basin. Other basins with similar structure and thick sediment accumulations are the Jiuquan basins (up to ~8 km thick); the Qaidam basin (up to 12 km in marginal foredeep, 5 km in basin center); the Ordos basin (up to 9 km of sediments in the western foredeep); and the Sichuan basin (up to 10 km thick in sedimentary deeps adjacent to foldbelts, only 1 km thick at thinnest places on platform part of the basin).

The major oil-producing basins in eastern China have a more conventional structure, with deep basin centers shallowing towards the margins. The Songliao basin of northeast China consists of a horst and graben structure, which is typical for all Chinese coastal and off-shore basins. Sedimentary thicknesses range from about 5 km on the uplifted structures (horsts), to over 7 km in the grabens. The sedimentary rocks thin out towards the margins. The Dian-Qian-Gui syneclise, located south of the Sichuan basin, contains the small Bose basin. The thickness of the sedimentary cover in some parts of the syneclise is up to 10 km. The Fuxin graben, located between the Songliao basin and the Bo Hai basin complex, contains up to 8 or 9 km of

sedimentary rocks, with interspersed igneous rocks. The Bo Hai basin complex contains as many as 87 separate and interconnected grabens. The sedimentary column from the Eocene to the present ranges in thickness from 7 to 10 km by itself. The thickness of the column here increases substantially if older rocks are included (for example, the late Precambrian carbonate platform is about 9.5 km thick; the Middle and Upper Jurassic is 8 to 10 km thick; the Tertiary can be up to 12 km thick).

Seismicity

Limited descriptions of earthquakes and associated damage are noted in the Chinese historical literature as far back as 1831 B.C., although these records are unevenly distributed in time and event location (Ma Xinguan, 1986, p. 32). Only after 1900 A.D. were field observations and instumental recordings (from stations outside China) made. Seismograph stations were not set up in China until after 1957 (Gu Gongxu, 1989).

Seismic events are widely distributed throughout China as seen on the map in Figure 10. Only the northern margin of China along the border with Mongolia, northeast China, the central part of the Tarim Basin, and the southeastern corner of China appear to be characterized by relatively lower levels of seismicity. These "quieter" areas are zoned for seismic intensity of less than VI, as indicated on the seismic intensity map of Figure 11. In correlating the two maps in Figures 10 and 11, it is seen that, in general, areas with a greater population of earthquake epicenters correspond, as expected, with areas zoned for higher seismic intensities.

During the past century, about 4,000 earthquakes with magnitudes greater than 4.7 occurred on mainland China and Taiwan; more than 50% of these events were located on Taiwan. Although the number of earthquakes on the Taiwan block is high, there are few earthquakes with high magnitudes (Ma Xingyuan, 1986, p. 34). On the mainland, frequent intracontinental earthquakes occur in the provinces of Xizang (Tibet), Xinjiang, Yunnan, western Sichuan, and Hebei. The number of earthquakes in these five provinces combined accounts for about 40% of the earthquakes in China. Although epicenters tend to be scattered throughout China, the larger events appear to be concentrated mostly in fault belts along the boundaries of crustal subplates and blocks. Ma Xingyuan (1986, p. 35) indicates that while data on focal depths of earthquakes are insufficient, almost 99% of earthquakes (presumably, ones for which focal depth estimates were made) are shallow crustal quakes. Ma Xingyuan (1986) also states that more than 90% of the earthquakes with magnitudes greater than or equal to 6.0 occur at depths between 10 - 25 km (the "seismogenic" layer of the Chinese literature).

Heat Flow

Heat flow data provide information on the thermal state of the crust. High heat flow may indicate zones of reduced crustal strength and increased seismic wave attenuation. Heat flow measurement data in China are sparse and distributed unevenly throughout the country, being concentrated mostly in the North China area. Some measurements are also available from southwest China, the northwest flank of the Sichuan basin, the Songliao basin of northeast China, and from south Xizang (Tibet). No data are available for the larger areas of northwest China and for much of the southeast coastal area.

The heat flow values in individual grids in the continental area of China range from 25 to 118 mW/m^2, exclusive of Xizang. The background ("normal") heat flow value for the continental area appears to be between 64 - 70 mW/m^2 (Huang and Wang, 1991b). The heat flow is up to 140 mW/m^2 in areas of Xizang; anomalously high heat flow in the Qinghai-Tibet plateau is also

indicated by volcanism and many active geothermal fields. (Heat flow values up to 245 mW/m^2 for lakes in Xizang are given by Wang and Huang, 1989, p. 585; these values do not appear to be repeated in more recent papers). Low velocity zones within the crust and upper mantle suggest that partial melting may be taking place in both the crust and upper mantle beneath the plateau (Zhang and others, 1984, p. 310). A map of China, on which the heat flow data are plotted on 1^0 x 1^0 grids, is given in Figure 12; the grid average values are taken to indicate the deep thermal state of the lithosphere (Huang and Wang, 1991b). The heat flow values for 22 regions in the continental part of China (see the numbered boxes on Figure 8, above) are summarized in Table 1.

A model of the crustal and upper mantle thermal structure is developed by Zaoxun Lu and others (1991) for the area of southern Liaoning, in northeast China, at the north end of Bo Hai (see Figure 13). This model is based on a series of geophysical investigations, mostly Deep Seismic Sounding (DSS) along the Luyang - Haicheng - Donggou profile. The model shows that in the zone from Guchengzi to Ximu the low velocity (and high conductivity) layer from 15 - 22 km depth in the crust is characterized by temperatures of 500 - 640^0 C, which is 130 - 200^0 C higher than for the crust on either side of this zone, at the same depth. The authors infer that this higher rate of heat generation may result from the presence of a relic intrusive body. The model also shows the temperature of the lithosphere is highest in the transition zone (i.e., the zone from the Lower Liaohe Plain to the Liaodong Peninsula); the temperature is lower in the Lower Liaohe Plain, and lowest on the Liaoning Peninsula, on either side of this transition zone. The temperature at the Moho is 720^0 C under the transition zone; it is 670^0 C beneath the Lower Liaohe Plain, and 600^0 C beneath the Liaodong Peninsula. The authors suggest that the Tancheng - Lujiang fault zone may be a deep seated fault which may serve as a conduit for heat transfer from the mantle. The heat flow value of the Moho discontinuity is 38 mW/m^2 beneath the Lower Liaohe Plain; 29 mW/m^2 beneath the Liaodong Peninsula; and 25 mW/m^2 beneath the transition zone. According to the authors, this low heat flow value at the Moho beneath the transition zone indicates that the heat flow value here is derived mostly from the high conductivity - low velocity layer in the crust. Addtionally, they indicate that the heat generation rate in the upper crust, along the whole profile, is not great, ranging from 1.05 x 10^{-12} J/cm^3 on the Liaodong Peninsula, to 1.47 x 10^{-12} J/cm^3 in the transition zone and the Lower Liaohe Plain; rates which are lower than those found in granites.

Salt Deposits

There are few data available on the depth, thickness, and geology of rock salt occurrences. As much as 80 to 90% of the commercially produced salt in China is derived from the solar evaporation of sea water along the coasts; 5 to 7% comes from inland salt brines, therefore, there has been little incentive to explore for salt in the interior. The map in Figure 14, after Werner (1988), shows the locations of "mines" in salt, though some of these locations, especially along the coast, are probably salt evaporation operations rather than mines in bedded salt. The basins discussed below are located on the map of petroleum basins in Figure 16.

Rock salt occurs in the Zigong area of Sichuan province, about 160 km southeast of Chengdu (mine number 8 in Figure 14). Yueh-Yen Lee (1942, p. 278) describes this deposit as being located in the axial portion of a structural dome, at a depth of about 840 meters. The salt occurs in an irregular lenticular form covering an area of about four km, with a maximum thickness of about eight meters. Robertson Research International Limited (1978, p. XII-3) describes the Chi-Liu-Ch'ing gas reservoir in the Sichuan basin as being capped by Middle Triassic evaporites (halite, anhydrite, and gypsum). The southeast and eastern parts of the basin are characterized by repeated folds which, according to Meyerhoff (1982, p. 239), are detatched; the entire area is one of large-scale decollement, presumably on salt.

More recently, occurrences of subsurface salt have been discovered during the course of hydrocarbon exploration in the various sedimentary basins of China. Diapiric salt domes are recorded in the Jianghan basin (Hubei province), and the Dongpu-Kaifeng and Jiyang depressions of the North China basin (Lee and Masters, 1988; Wang Xie-Pei and others, 1985).

In the Jianghan basin, Xie Taijun and others (1988) indicate that salt occurs only in the Qianjiang, Xiaoban, and Yunjin depressions in the eastern part of the basin. There were two periods of salt deposition in the basin; the earlier period was from Cretaceous apparently through Paleocene and Early Eocene time; the later period was from Late Eocene to Early Oligocene time. The maximum thickness of salt is given as 1,800 meters. In the Qianjiang depression, the salt is up to 1,265 meters thick. Salt structures in this depression include salt domes and anticlines, as seen in Figure 15.

The Early Tertiary section in the Dongpu-Kaifeng depression of the North China basin is described by Lee (1986, p. 12, 32) as consisting of 400 to 2,000 meters of mudstone and siltstone intercalated with salt beds, gypsum beds, and shale. Zhu Jiawei and Xu Huazheng (1988) describe two layers of Tertiary salt and gypsum in the Wenliu gas field of the Dongpu depression. The upper layer occurs at depths of about 3,500 to 4,000 meters on the flank of the dome structure; the lower layer occurs at depths of about 4,300 to 5,000 meters. Apparently only the lower salt layer occurs on the dome structure, at depths of about 2,000 to 2,600 meters. Here, the salt is 600 to 800 meters thick. Two layers of Tertiary salt also occur in the Wei-chen gas field of this depression. Here, the upper salt layer occurs at depths of about 2,300 to 2,600 meters; the lower layer occurs at about 2,500 to 3,000 meters depth.

Additionally, the presence of salt is mentioned in several other areas, but no details are currently available. Salt and gypsum deposits are indicated in the Miocene section in the central and eastern parts of the Qaidam basin. Miocene bedded anhydrite and halite are noted in the Turpan basin. In the Mekong foldbelt in Yunnan province, occasional salt beds are described in the Lower Jurassic section (Robertson Research International Limited, 1978; Jackson and Talbot, 1991). Lower Ordovician salt and anhydrite has also recently been described in the Ordos basin (C. D. Masters; G. Ulmishek, oral communication, 1993; Yi Shiwei, 1992) where it occurs in several thin layers throughout the sedimentary section, with the greatest cumulative thickness of about 300 meters indicated in one well section. Finally, the Chinese have mentioned a 600 meter thick salt section in the northern Tarim basin, east of the more recent oil discoveries (G. Ulmishek, oral communication, 1993), but this has not been substantiated in the literature. The descriptions of salt deposits found in the literature appear to suggest that, in most instances, the salt beds are thin and are often interbedded with other rock types. Only a couple of descriptions suggest the possibility of thicker salt deposits (Jianghan basin; North China basin; possibly the eastern Tarim basin). This may reflect the general lack of data on salt, as available in the Chinese literature. The data collected on the known salt deposits are summarized in Table 2.

Oil and Natural Gas Development

The use of petroleum in China dates back to 3000 B.C. or earlier. About 600 B.C., bamboo wells were drilled in the Sichuan basin for salt brines, which produced associated gas. In 211 B.C., a gas well was drilled in limestone, on an anticlinal structure west of Chungking. By 1900, more than 1,100 wells had been drilled on this structure. In addition to bamboo drilling, shallow gas wells were also dug by hand (Meyerhoff, 1978, p. 272). Some of the early discoveries of gas were found at depths of less than 100 m.

Oil and natural gas are now found in sedimentary basins scattered throughout China (see the map of distribution of major oil fields and producing basins, in Figure 16). By 1978, 30 basins were known on the mainland and offshore regions of China (Meyerhoff, 1978, p. 309). At least

145 oil and gas fields have been discovered in these basins, 85 of which were productive by 1978. As of 1988, 14 major basins were productive onshore, 3 basins were productive offshore (Lee and Masters, 1988). Petroleum reservoirs are known in rocks from all of the geologic time periods, and in a wide variety of rock types, including metamorphic and volcanic rocks. The main reservoir rocks are Upper Mesozoic to Cenozoic sandstones. Some reservoirs are characterized by porosities as high as 20 - 35% and permeabilities up to hundreds of millidarcies to a few darcies; other reservoirs (particularly those in the Sichuan basin) are tight, with porosities only on the order of 1 - 3%. In these reservoirs, increased porosity from fractures is important in oil production. Outside of the producing fields the rocks are, in general, characterized by very low porosity and permeability. Most of the fields in China produce oil from non-marine sources. The main gas fields are limited to the Sichuan and Qaidam basins. Some gas fields are noted in the Dongpu-Kaifeng depression of the North China basin; one field each is noted in the Tarim and Junggar basins, and gas deposits are noted in the more recent work on the Ordos basin (Yi Shiwei, 1992).

Relatively high geothermal gradients in the sedimentary basins (3^0 C/100 m to 5^0 C/100 m in the eastern regions) result in reservoir temperatures commonly in the 100^0 to 150^0 C range (Masters and others, 1980). These higher temperatures found at relatively shallow depths indicate that the oil-generation window is at shallow depths, which explains the occurrence of many oil pools at 1,000 to 3,000 m depth in the eastern China basins (K. P. Wang, 1975, p. 29; Masters and others, 1980), while the deposits in western China are usually more than 5,000 m deep (U.S. Dept. of the Interior, 1993, p. 88).

Increased exploration activity and recent discoveries in the western basins (especially the Tarim and Junggar basins) indicate a high level of interest in these areas, where significant future discoveries are anticipated. Western oil companies have participated in exploration of the offshore basins on the continental shelf, in the South and East China Seas, in which significant petroleum reserves are also anticipated.

Mining Regions

China is the worlds's largest producer of bituminous and anthracite coal, which is the country's most important source of primary energy. It is produced in many provinces in the north, northeast, and southwest parts of the country (see the map of distribution of coal deposits in China, in Figure 17), with Shanxi province being the leading producer. Some of the richest coal resources are located in Shaanxi province and the western part of Nei Monggol (U.S. Department of the Interior, 1993). More than 95% of the coal in China was formed in the Carboniferous, Permian, and Jurassic periods; coal is also known from the Triassic, Early Cretaceous, and Tertiary periods. Proven reserves are mostly bituminous and anthracite, but also include coking coal and lignite (Dorian and Fridley, 1988; Worden and others, 1988; Werner, 1988). Much of the coal produced in China is of low quality, containing a high ash content. Although about 80% of the known deposits are in the north and northwest parts of the country, most of the mines are located in Heilongjiang province (northeast China) and the eastern part of China because of their proximity to the regions of highest demand (Worden and others, 1988, p. 324).

Geological explorations in China have revealed economic deposits of over 130 mineral and energy commodities. China is ranked number one in world production of coal and hydraulic cement; number two in salt and nitrogen; number three in manganese and iron ore, and number four in crude oil, oil refinery products, phosphate rock, crude steel, tin and zinc (U.S. Dept. of Interior, 1990a). With the discovery of the Bayan Obo deposit in North China, the country is now a leader in the production of rare earth elements (REE). Additionally, China is among the world leaders in proven deposits of tungsten, antimony, molybdenum, vanadium, titanium, pyrite, gypsum, barite, copper, lead, aluminum, mercury, nickel, niobium, asbestos, fluorite, magnesite, tantalum, lithium, bauxite, and borax. Other natural resources include natural gas, magnetite, and

hydropower (CIA, 1989; Clark and others, 1985). The maps in Figure 18 show the distribution of metallic and non-metallic minerals in China.

China is also rich in uranium and has favorable geological conditions for the formation of uranium deposits (Worden and others, 1988). The four main types of uranium deposits in the country are granite, volcanic, sandstone, and carbonaceous-siliceous-pelitic rock. Precambrian metasomatite uranium deposits also occur. The map in Figure 19 shows the location of known uranium deposits, the uranium provinces in which they occur, and the geologic type of deposit.

Karst

Carbonate rocks (limestone and dolomite) exposed on the earth's surface cover an area of about 907,000 km^2 in China, and range in age from Precambrian to Cenozoic. Buried carbonates (i.e., those underlying non-soluble rock) and covered carbonate rocks (i.e., those overlain by unconsolidated sediments usually 10 to 50 meters thick) cover about 3,443,000 km^2, approximately one third of China (Yuan Daoxian, 1992). The distribution of carbonate rocks in China is shown on the map in Figure 20. Although karst often develops in carbonate rocks, the occurrence of carbonates does not necessarily require the presence of karst everywhere in those rocks. For example, carbonates occur extensively on the Tibet Plateau and, although some karst features do occur here, they are not well developed because tectonic uplift of the area resulted in a relatively cold and dry Quaternary period in this region. In general, the carbonate areas in the western parts of the country are characterized by poorly developed karst landforms, although shafts and caves are known in the Chinghai mountains of Gansu and in the Tien Shan mountains of Xinjiang (Middleton and Waltham, 1986, p. 56).

The carbonate regions of eastern China are dominated by the Yunnan and Guizhou plateaus, and the Guangxi plains, famous for its tower karst. The Yunnan-Guizhou plateau measures hundreds of kilometers across, and contains hundreds of caves (Middleton and Waltham, 1986). In southeastern China (in the Guizhou karst), the carbonate sequence is as much as 3,000 to 10,000 meters thick, and ranges in age from late Precambrian to Ordovician, and from Devonian to Triassic (Yuan Daoxian, 1992). The greatest cave potential is in the marginal areas of the Guizhou plateau; the greatest depth potential for caves is in the higher parts of the plateau in western Guizhou and eastern Yunnan. A chamber in the Gebihe cave of Ziyun County, Guizhou Province, is described as the second largest in the world, after the Sarawak Chamber in Malaysia. This room, called the Miao Chamber, measures 700 m long by 200 m wide and 40 to 100 m high, with an area of 116,000 m^2 (Zhang Shouyue, 1993). To the south of the Guizhou plateau, the carbonates in the Guangxi region make up the major solutional plain in the country. The lower elevations of these plains and hills contain the world's largest area of tower karst, where many isolated limestone peaks rise abruptly from the surrounding plain, as remnants of long-term lateral dissolution of a thick, extensive carbonate sequence. Caves are common throughout this region. Underlying the plain is a karst aquifer which, when overpumped, may cause surface collapses (Middleton and Waltham, 1986; Yuan Daoxian, 1992).

North of the Yunnan-Guizhou plateaux the carbonates and the karst landforms are less well developed. In northern China, the carbonates are 1,000 to 5,000 meters thick, and extend from the late Precambrian to Middle Ordovician. These flat-lying rocks accommodate many major karst hydrologic systems, each one covering hundreds to thousands of square kilometers in area (Yuan Daoxian, 1992).

The major occurrences of buried karst in China are in the Sichuan Basin and North China Plain. In the Sichuan Basin, karstic carbonate rocks of Precambrian to Triassic age are buried under hundreds to thousands of meters of Mesozoic red beds. In oil and gas wells drilled to depths of

1,000 to 3,000 m, caves to 4 or 5 m in diameter are often encountered in Permian or Triassic limestones. In the North China Plain, Precambrian to Middle Ordovician-aged carbonate rocks, in which caverns are occasionally encountered, are buried under thousands of meters of Cenozoic rocks. In buried karst systems, the groundwater is usually characterized by high total dissolved solids (100 - 300 g/l) and high temperature (about 100^0 C), indicating a relatively closed system (Yuan Daoxian, 1992).

In addition to the landforms developed in the carbonate rocks of China, karst features are also noted in salt and gypsum in several areas of the northwest, and also in sandstone at Qingyan, in Hunan. Also, caves are known in the basalts of Wudalainzhi region of Manchuria (Middleton and Waltham, 1986, p. 56).

Loess

The overall areal distribution of loess in China is significant, but the greatest thickness of about 200 meters has a very limited distribution. Although this thickness is insufficient for fully decoupling even a small (1 kt) explosion, loess is considered here because of its potential to partially decouple, or attenuate, a seismic signal from a small explosion detonated in this environment, in a manner similar to that of the thick unconsolidated sequence at the U.S. test site in Nevada. The most favorable region for such a scenario is the southern margin of the loess plateau (see Figures 21 and 22) where the highly porous, unconsolidated material attains its maximum thickness of over 200 meters. Some of the loess on the southern margin of the plateau is drained by underlying karstic limestone, further adding to the decoupling potential of loess in this area.

Loess is generally considered to be a wind-blown deposit, consisting mostly of silt-sized particles (0.075 - 0.002 mm diameter), with lessor amounts of fine sandy and clayey materials. Although the mineral composition of loess varies considerably from area to area, the constituent minerals are usually mostly quartz (more than 60%) which together with feldspars, micas, and carbonates, make up about 90% of the composition. The carbonate content, of both primary and secondary origin, ranges from less than 4% to about 28%. Heavy minerals (most commonly epidote, amphibole, hematite, limonite, garnet, and zircon) make up about 4% as medium- to coarse-grained silt and sand. There is also a small amount of organic material (Derbyshire, 1983; Liu, 1988; and Zhang and others, 1991).

The physical properties of loess are variable, but in general it is characterized by high porosity and low bulk density. Porosities range from about 10% to over 55%, averaging 45% to 50%. Average dry bulk densities range from about 1.4 to 1.6 g/cm^3. The grain density of loess is estimated to approximate the grain density of quartz (2.65 g/cm^3), which is the main constituent of loess. Upon natural collapse of the loess, due to subsidence, the reduction in the void ratio may be as much as 25%, giving a coefficient of subsidence of as much as 10% (Liu, 1988; and Derbyshire, 1983).

The distribution of loess is widespread in China, as seen on the map in Figure 21. Loess deposits are found from the area of the Tien Shan and Altai Mountains in northwestern China, through north-central China, and extending to the region around Harbin in the northeastern part of the country. In China, loess covers a total area of about 631,000 km^2. The greatest occurrence of loess in the world is found in the Loess Plateau in the north-central part of the country, located between 34^0 to 41^0 N x 102^0 to 114^0 E, and covering about 440,000 km^2 (Zhang and others, 1991). Here, most of the loess has accumulated in the middle reaches of the Huang He (Yellow River). The greatest known thickness of loess in the world occurs near the city of Lanzhou, where it is about 410 m thick (Zhang and others, 1991). The variable thickness of the loess in the area of

the Loess Plateau is demonstrated on the map in Figure 22. In this area, as well as in the rest of the country, the thickness of loess varies, depending on the geomorphology of the underlying bedrock and location of deposition, thinning in some areas to several meters or less. Interbedded layers of fossil soils, and zones with carbonate concretions are locally common in the loess, especially in the thicker sequences.

The occurrence and distribution of groundwater in loess is influenced by precipitation and evaporation rates, thus the depth to water fluctuates between the summer months and the winter months. Migration of groundwater within the loess is strongly controlled by the anisotropic nature of the structure and permeability of loess, with the result that the depth to groundwater is variable even over short distances. The geomorphology of the loess deposit also influences the depth to groundwater. In wide, flat-bottomed valleys filled with loess, the depth to water may be relatively shallow, ranging from several meters to more than 10 meters depth. The depth to water in the flat-topped tablelands and rounded hills composed of loess may range from about 25-30 meters in the center, increasing to 70 meters or more at the margins. The groundwater is contained in fractures and fissures, which are commonly vertically oriented; in the intergranular pore spaces; as well as cavities developed locally in carbonate concretions and the loess itself. These irregularly shaped cavities are generally 1-2 cm, up to 5 cm on the long axis. The development of fissures, pores, and permeability decreases with increasing depth in the loess. Because of differences in precipitation rates, water is less abundant in loess in the northern parts of the Loess Plateau due to lower precipitation, whereas further south, where precipitation is greater, the groundwater is more abundant and occurs at shallower depths. In some areas (for example, the northeast margin of the Wei River basin), the loess lies directly on karstic limestone, which drains the groundwater from the loess. The thickest occurrences of *unsaturated loess* are therefore likely to occur in areas underlain by karstic limestone. Periods of rapid ground water recharge can cause large-scale headward erosion, resulting in subsurface tubes or channels, called *loess karst*. This rapid subsurface erosion probably causes the surface collapse and subsidence features associated with loess deposits (Derbyshire, 1983; and Research Group..., 1976).

References

Arora, S. K., and Basu, T. K., 1984, A source discrimination study of a Chinese seismic event of May 4, 1983, Tectonophysics, no. 109, p. 241-251.

Cao Jiadong, and Shao Shixong, 1991, Neotectonic movements in China, in: The Quaternary of China Chief ed. Zhang Zonghu, XIII INQUA, China Ocean Press, p. 9-41.

Central Intelligence Agency, 1979, China, shaded relief base map, scale 1:10,000,000.

Central Intelligence Agency, 1989, The world factbook 1989, CPAS WF 89-001, May 1989, 367 p.

Che Yongtai, 1987, Response of ground water levels in wells to underground nuclear explosions, (in Chinese), Shuiwendizhi Gongchengdizhe (Hydrology and engineering geology), no. 4, p. 7-12.

China Today, 1988: Nuclear Industry, Part II, translated in FBIS, JPRS Report, Science and Technology, China, JPRS-CST-88-008, April 26, p. 59-81.

Chu Yucheng, 1986, Observations of unstable rock mass under underground nuclear explosions (in Chinese), Chengdu Baozha Yu Chongji (Explosions and shockwaves), no. 6, p. 261-267.

Clark, A. L., Dorian, J. P., and Fan, P. F., 1985, An estimate of the mineral resources of China, Resource Systems Institute, working paper WP-85-5, Honolulu, 60 p.

Compiling committee of seismic zoning map in China, 1992, Seismic intensity zoning map of China (1990) and its explanations, Earthquake research in China, vol. 8, no. 4, p. 1-11.

Cuellar, G., and Shen Xian-jie, 1993, UN project document signed, Chinese-Italian energy project for China, Geothermal Resources Council, Bulletin, vol. 22, no. 9.

Das, S., and Filson, J. R., 1975, On the tectonics of Asia, Earth and Planetary Science Letters, vol. 28, p. 241-253.

Derbyshire, E., 1983, On the morphology, sediments, and origin of the Loess Plateau of central China, in: Mega-Geomorphology, R. Gardner and H. Scoging, eds., Clarendon Press, Oxford, p. 172-194

Ding Zemin (Chief ed.), 1987, Irrigation and drainage in China, Ministry of Water Resources and Electric Power, P.R.C., China Water Resources and Electric Power Press, Beijing, 111 p.

Dorian, J. P., and Fridley, D. G., (eds.), 1988, China s energy and mineral industries, current perspectives, Westview special studies in natural resources and energy management, Westview Press, Boulder/London, 162 p.

Fieldhouse, R. W., 1991, Chinese nuclear weapons: a current and historical overview, Natural Resources Defense Council, Nuclear Weapons Databook, working papers, Washington, D.C., 77 p.

Finch, W. I., Feng, S., Zuyi, C., and McCammon, R. B., (eds.), 1993, Descriptive models of major uranium deposits in China, in: Non-renewable resources, vol. 2, no. 1, Spring, 1993, for: International Association for Mathematical Geology, Oxford University Press, p. 39-49

Geng Shufang, and Fan Benxian, 1990, Geological map of China (postcard).

Gu Gongxu, (chief ed.), 1989, Catalogue of Chinese earthquakes (1831 B.C. - 1969 A.D.), Science Press, Beijing, 872 p.

Huang Shao-peng, and Wang Ji-yang, 1991a, Several heat flow values from deep drill holes in the northwest depression of the Sichuan basin, SW China, Chinese Science Bulletin (Kexue Tongbao), Chinese Academy of Sciences, Beijing, vol. 36, no. 1, p. 47-51.

Huang Shaopeng, and Wang Jiyang, 1991b, On variations of heat flow and Pn velocity - a case study from the continental area of China, Journal of geodynamics, vol. 13, no. 1, p. 13-28.

Institute of hydrogeology and engineering geology, 1976, Karst in China, Chinese Academy of Geological Sciences, Shanghai Peoples Publishing House

Jackson, M. P. A., and Talbot, C. J., 1991, A glossary of salt tectonics, Bureau of Economic Geology, The University of Texas at Austin, Geological Circular 91-4.

Jiao Shuqin, 1985, Groundwater in China, in: Hydrogeological mapping in Asia and the Pacific region; Proceedings of the ESCAP-RMRDC workshop, Bandung, 1983; International Contributions to Hydrology, vol. 7, ed. by G. Castany, E. Groba, and E. Romjin, Heise, Hannover, p. 91-119.

Karst Research Team, Institute of Geology, 1979, Karst research in China, Academica Sinica, Academic Press, 336 p.

Lang, W. J., and Sun, R. J., 1966, Atlas of Asia and Eastern Europe to support detection of underground nuclear testing, Vol. III., Seismicity, prepared by Dept. of the Interior, U.S. Geological Survey, for Advanced Research Projects Agency.

Lee, K. Y., 1986, Geology of the petroleum and coal deposits in the North China basin, eastern China. Department of the Interior, U.S. Geological Survey, Open-File Report 86-154, 57 p.

Lee, K. Y., and Masters, C. D., 1988, Geologic framework, petroleum potential, and field locations of the sedimentary basins in China, Department of the Interior, U.S. Geological Survey, Miscellaneous Investigation Series, Map I-1952, scale 1:5,000,000.

Liu Tungsheng, 1988, Loess in China, 2nd. ed., Springer-Verlag Series in Physical Environment, Springer-Verlag, 224 p.

Lu Yan, 1980, Physical geological reactions to underground nuclear explosions, Shuiwendizhi Gongchendizhi (Hydrology and Engineering Geology), no. 5.

Ma Xingyuan (chief compiler), 1986, Explanatory notes for the lithospheric dynamics map of China and adjacent seas, scale 1:4,000,000, Geological Publishing House, Beijing, 53 p.

Ma Xingyuan (chief editor), 1989, Lithospheric dynamics atlas of China, China Cartographic Publishing House, Beijing, 69 plates.

Masters, C. D., Girard, Jr., O. W., and Terman, M. J., 1980, A perspective on Chinese petroleum geology, U.S. Department of the Interior, Geological Survey, Open-File Report 80-609, 21 p.

Melnikov, N. V., 1975, (ed.), Spravochnik (Kadastr) fizicheskikh svoitsv gornykh porod (Handbook [Cadaster] of physical properties of rocks), Nedra, Moscow, p. 262.

Meyerhoff, A. A., 1978, Petroleum exploration in the Soviet Union and China, 9th Annual Canadian Society of Petroleum Geologists Seminar, Dept. of Geology, The University of Calgary, Calgary, Alberta, Canada, p. 259-375.

Meyerhoff, A. A., 1982, Petroleum basins of the Union of Socialist Soviet Republics and the Peoples Republic of China and the politics of petroleum, course notes, Petroleum Exploration Society of Australia, Distinguished Lecture Series, 341 p. plus 141 figures.

Meyerhoff, A. A., Kamen-Kaye, M., Chen, C., and Taner, I., 1991, China - stratigraphy, paleogeography and tectonics, Kluwer Academic Publishers, the Netherlands.

Middleton, J., and Waltham, T., 1986, The underground atlas, a gazetteer of the worlds cave regions, St. Martins Press, New York, 239 p.

Molnar, P., Fitch, T. J., and Wu, F. T., 1973, Fault plane solutions of shallow earthquakes and contemporary tectonics in Asia, Earth and Planetary Science Letters, vol. 19, no. 2, p. 101 - 112.

Research Group of the Hydrology of Loess in the Middle Reaches of the Yellow River, 1976, On the hydrology of loess in the middle reaches of the Yellow River, Peking, 14 p.

Revenaugh, J., and Sipkin, S. A., 1994, Mantle discontinuity structure beneath China, Journal of Geophysical Research (Solid Earth), vol. 99, no. B-11, p. 21,911-21,927.

Robertson, E. C., 1989, Report on explosion effects on granite and limestone in dry-warm and wet-cold environments, (February), (unpublished manuscript for MGP, USGS), 5 p.

Robertson Research International Limited, and Bureau d Etudes Industrielles et de Cooperation de l Institut Francais du Petrole, 1978, The People s Republic of China: Its petroleum geology and resources, Robertson Research Group.

Shao Shihxiong, Zhang Yufang, and Han Shuhua, 1982, Lithologic characters of the Quaternary volcanic deposits and time division of the volcanic activities in Hebei Plain, China, in: Quaternary Geological Research, Papers of Chinese geologists submitted to XI INQUA Congress, Beijing, p. 5-1 - 5-10.

Tapponnier, P., and Molnar, P., 1979, Active faulting and Cenozoic tectonics of the Tien Shan, Mongolia, and Baykal regions, Journal of Geophysical Research, vol. 84, p. 3425-3459.

Terman, M. J., Bowers, W. E., Soleimani, G., and Woo, C. C., 1974, Tectonic map of China and Mongolia, compiled for Advanced Research Projects Agency , Geological Society of America, 2 sheets.

Ulmishek, G., 1992, Geology and hydrocarbon resources of onshore basins in eastern China, Department of the Interior, U.S. Geological Survey, Open File Report 93-4, 150 p.

United Nations, 1986, Ground water in continental Asia (Central, eastern, southern, south-eastern Asia), Department of Technical Cooperation for Development, Natural Resources/Water Series No. 15, ST/ESA/157, p. 76-97.

United States Department of the Interior, 1990a, U.S. Bureau of Mines, MineralsYearbook, Vol. III, 1988, Area Reports: International, U.S. GPO, Washington, D.C., 1126 p.

United States Department of the Interior, 1990b, Geological Survey, Global hypocenter data base CD-ROM

United States Department of the Interior, 1993, Mineral industries of Asia and the Pacific, Minerals yearbook, vol. III, 1991 International review, Bureau of Mines, U.S. GPO, Washington, D. C., 404 p.

Wang Hongzhen, 1986, The tectonic framework and the geotectonic units, in: The geology of China, Yang Zunyu, ed., Clarendon Press, Oxford, p. 237-255.

Wang Ji-yang, and Huang Shao-peng, 1989, Statistical analysis of continental heat flow data from China, Chinese Science Bulletin (Kekue Tongbao), Chinese Academy of Sciences, Beijing, vol. 34, no. 7, p. 582-587.

Wang Ji-yang, and Xiong Liang-ping, 1989, Groundwater flow and geotemperature pattern, in: Beck, A. E., Garven, G., and Stegena, L., (eds.), Hydrological regimes and their subsurface thermal effects, Geophysical Monograph 47, IUGG Vol. 2, p. 87-99.

Wang, K. P., 1975, The People s Republic of China - a new industrial power with a strong mineral base, Bureau of Mines, U.S. Department of the Interior, U.S. GPO, Washington, D.C. 96 p.

Wang Xie-Pei, Fei Qi, and Zhang Jia-Hua, 1985, Cenozoic diapiric traps in eastern China, The American Association of Petroleum Geologists Bulletin, vol. 69, no. 12, p. 2098-2109.

Werner, A., 1988, The mineral industry of China, statistics and locations, Energy, Mines and Resources Canada, 112 p.

Worden, R. L., Savada, A. M., and Dolan, R. E., (eds.), 1988, China, a country study, 4th. ed., U.S. GPO, Washington, D.C. 732 p.

Wu Gongjian, and Yu Pan, 1987, Types of China s crust and their geophysical characteristics (abs. II), International symposium on tectonic evolution and dynamics of continental lithosphere, The third all-China conference on tectonics, Beijing, China, 157 p.

Xie Taijun, Wu Lizhen, and Jiang Jigang, 1988, Oil and gas fields in the Jianghan Basin, Hubei Province, China, in: Wagner, H. C., Wagner, L. C., Wang, F. F. H., and Wong, F. L., (eds.), Petroleum resources of China and related subjects; Houston, Texas, Circum-Pacific Council for Energy and Mineral Resources Earth Science Series, V. 10, . 345-358.

Yi Shiwei, 1992, Development of Mizhi intra-platform depression and its gas potential, Oil and gas geology, (in Chinese), vol. 13, no. 3, p. 293 -302.

York, J. E., Cardwell, R., and Ni, J., 1976, Seismicity and Quaternary faulting in China, Bulletin, Seismological Society of America, vol. 66, no. 6, p. 1983-2001.

Yuan Daoxian, 1992, Karst and karst water in China, in: Hydrogeology of selected karst regions, International Association of Hydrogeologists, International Contributions to Hydrogeology, H. Paloc and W. Back, eds., vol, 13, p. 315-338.

Yueh-Yen Lee, 1942, Geochemical interpretation on the salt deposits in Szechuan, Bulletin of the Geological Society of China, vol. 22, nos. 3-4, p 277-291.

Zaoxun Lu, Guodong Liu, Menghua Wei, Puzai Meng, and Junmeng Zhao, 1991, Lateral inhomogeneity of crust and upper mantle in southern Liaoning, China and its relationship with the M = 7.3 Haicheng earthquake, Acta Seismological Sinica, distr. by Pergamon Press, vol. 4, no. 4, p. 521-534.

Zhang Shouyue, 1993, Grand caves of China, Proceedings of the XI International congress of speleology, August 2 to 8, 1993, Beijing, China, Interanational Union of Speleology, p. 236-239.

Zhang Yufang, 1991, Quaternary volcanic activity in China, in: The Quaternary of China, XIII INQUA Congress, Zhang Zonghu, Chief ed., China Ocean Press, p. 274 - 306.

Zhang, Zh. M., Liou, J. G., and Coleman, R. G., 1984, An outline of the plate tectonics of China, Geological Society of America, Bulletin, vol. 95, no. 3, p. 295-312.

Zhang Zonghu; Zhang Zhiyi; and Wang Yunsheng, 1991, Loess in China, in: The Quaternary of China, XIII INQUA Congress, Zhang Zonghu, Chief ed., China Ocean Press, p. 459-508.

Zheng Jiandong, 1991, Significance of the Altun Tagh fault of China, Episodes, vol. 14, p. 307-312

Zhu Jiawei, and Xu Huazheng, 1988, Geochemical characteristics of natural gas in the Dongpu depression, North China, in: Wagner, H. C., Wagner, L. C., Wang, F. F. H., and Wong, F. L., (eds.), Petroleum resources of China and related subjects: Houston, Texas, Circum-Pacific Council for Energy and Mineral Resources Earth Science Series v. 10, p. 535-545.

Figure 1. Simplified geological map of China, showing the distribution of granitic, basaltic, sedimentary, and metamorphic rocks of various ages. (Geng Shufang and Fan Benxian, 1990).

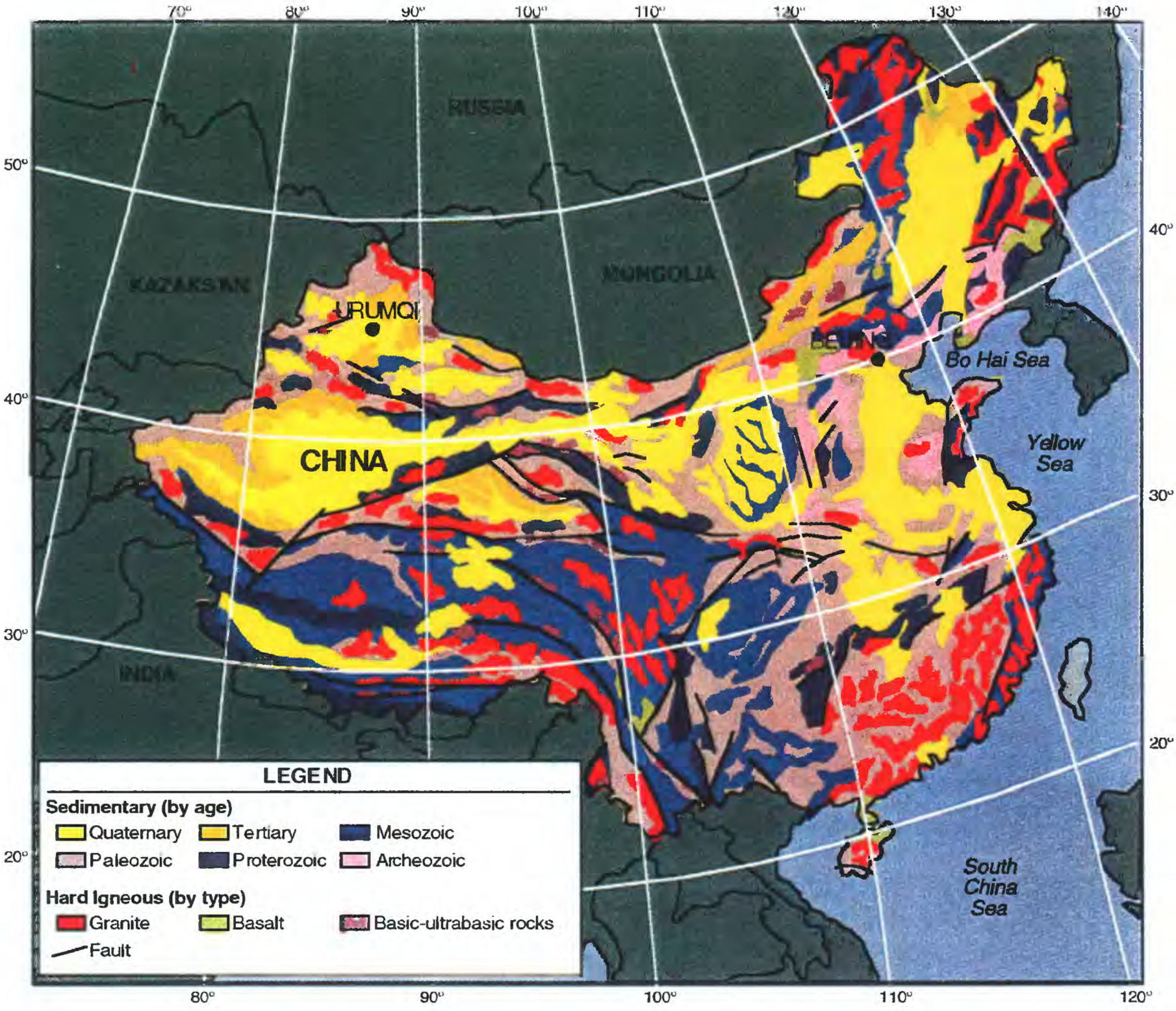

Figure 2. Map of distribution of precipitation throughout China. The desert areas of northern and northwest China, which receive less than 200 mm annual precipitation, are highlighted in white. These are the areas with potential for thick, dry, unconsolidated materials. (Ding, 1987).

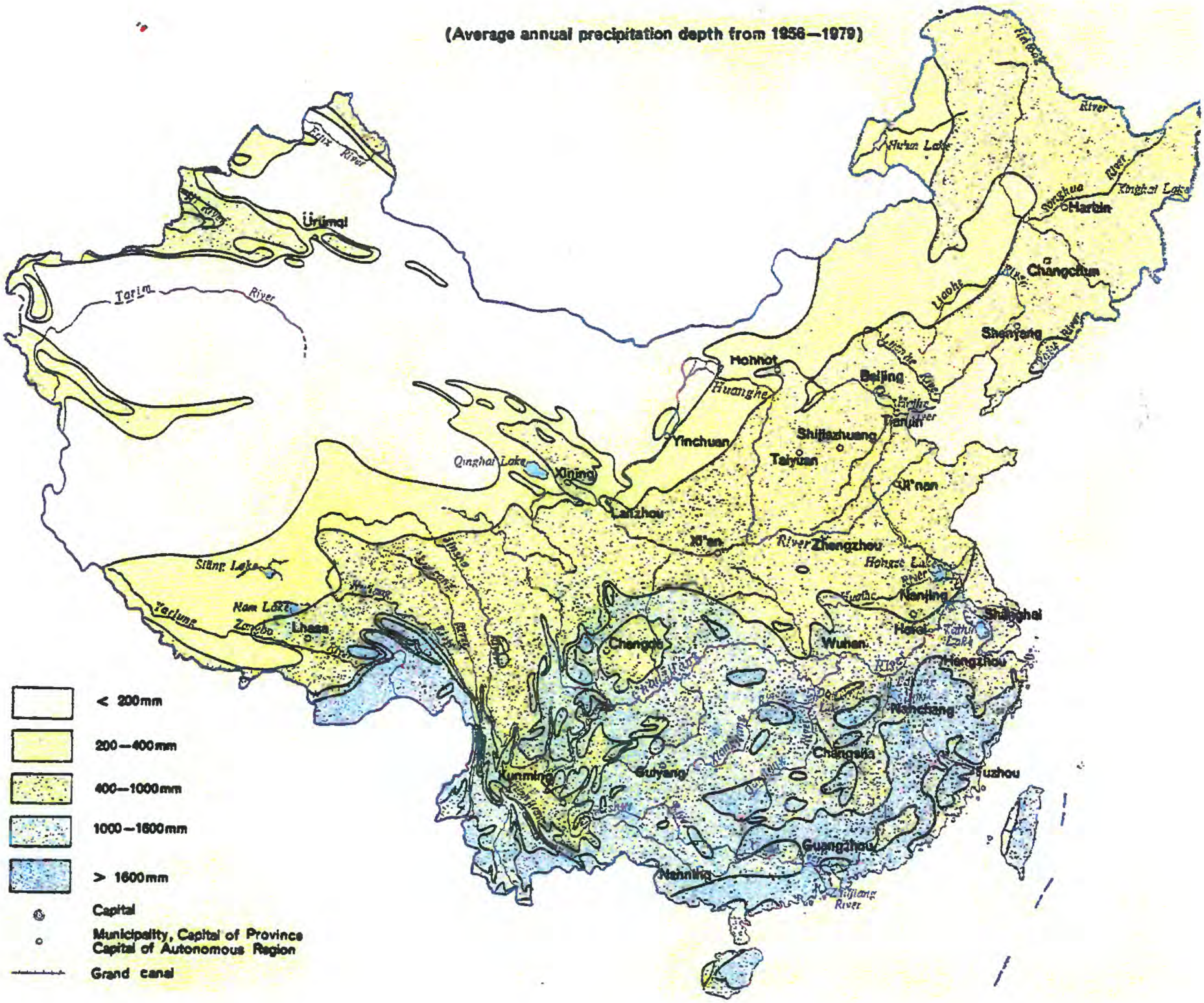

Figure 3. Simplified tectonic map of China. The principal tectonic regions are from Terman and others, 1974. Significant subregions, discussed in the text, are added. The North China (Tarim) - Korean and South China platforms are the main tectonic elements of the Chinese mainland, which are surrounded by various fold systems.

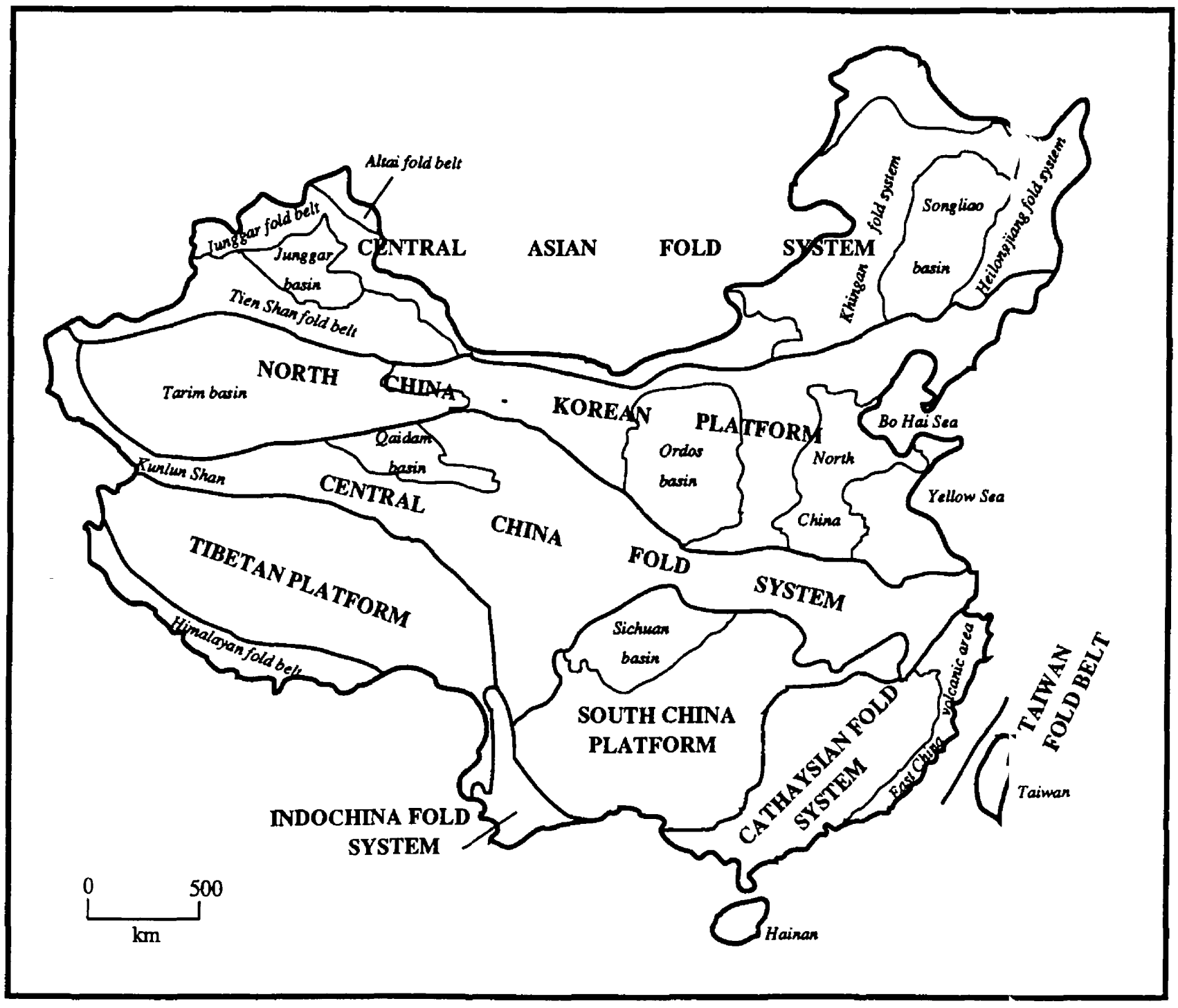

Figure 4. Major active fault belts in China, with associated focal mechanism solutions. The shaded portions of the solutions are the compressional quadrants, the orange portions are the dilational quadrants. (From Ma Xingyuan, 1989).

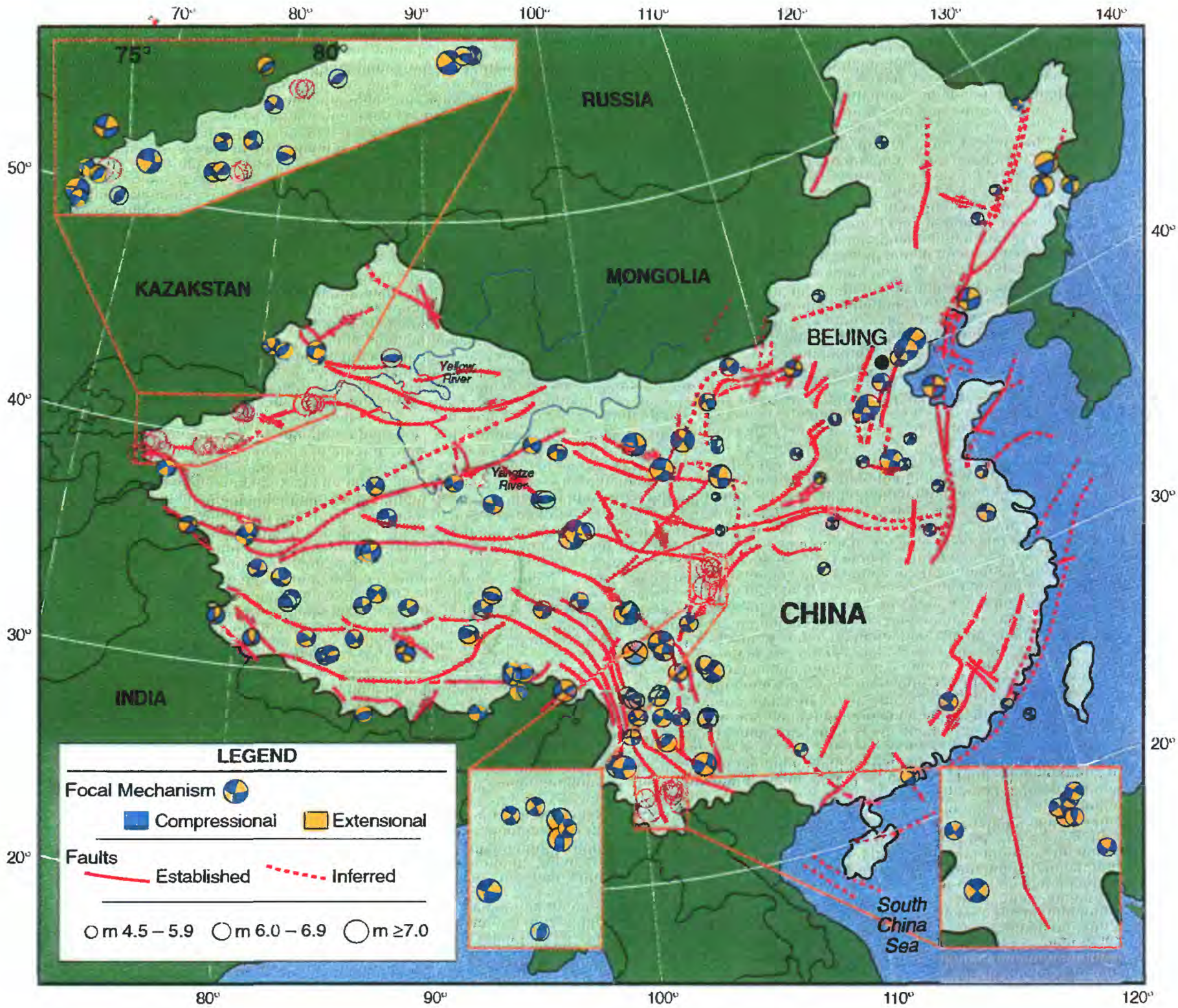

Figure 5. Model of the recent tectonic stress field in China and adjacent areas. (After Ma Xingyuan, 1986).

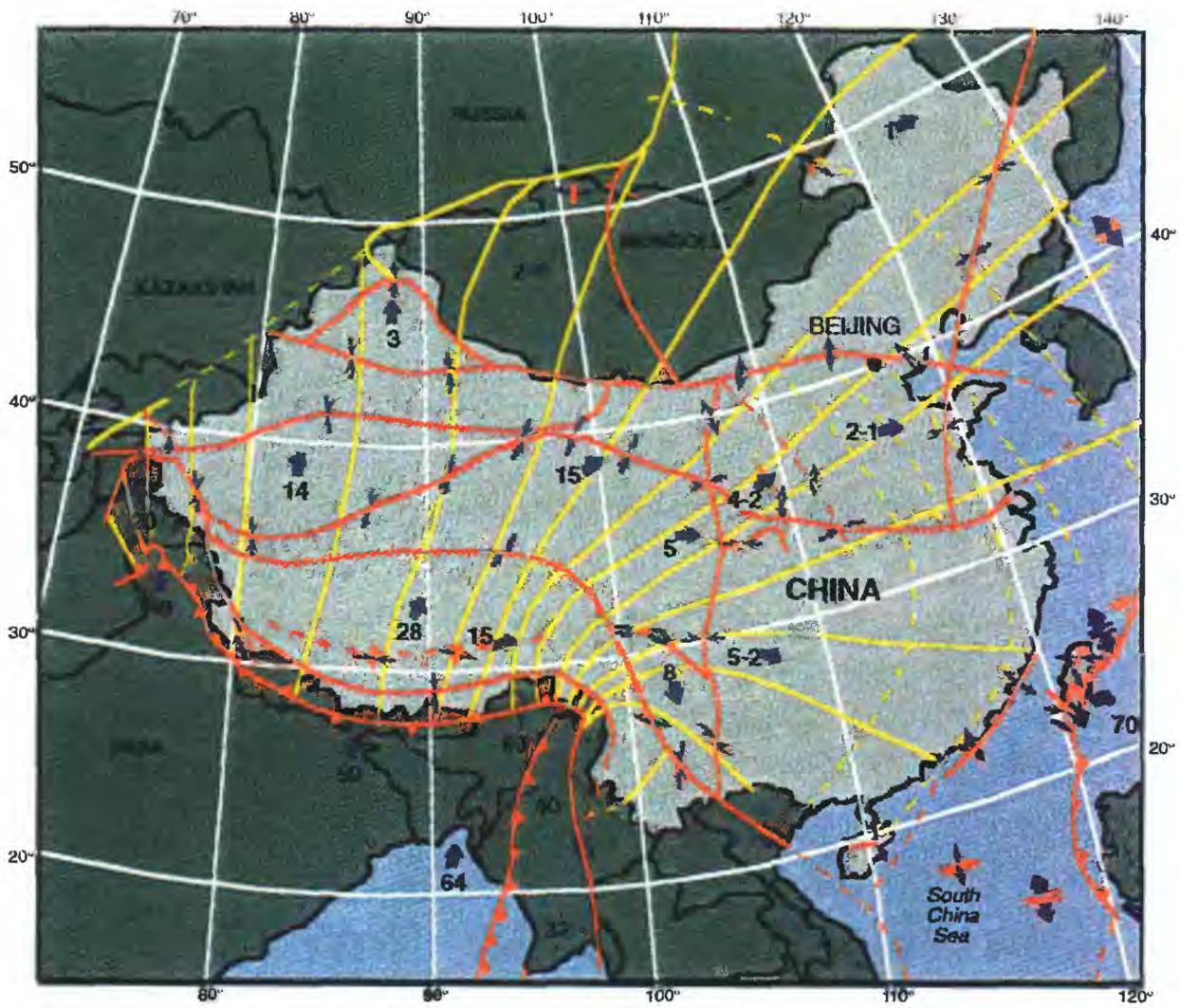

LEGEND

Relative motion vectors and rates of active plates (mm/yr)

- Divergent
- Subduction
- Collision
- Transform boundaries

- Relative motion vector of subplates and blocks
- Intraplate graben and rift
- 50 — Relative motion vector of subplates and blocks with respect to the Eurasian plate (Siberian craton) and rates (mm/yr)
- Trajectory of maximum compressional principal stress axis
- Trajectory of minimum principal (tensile) stress axis

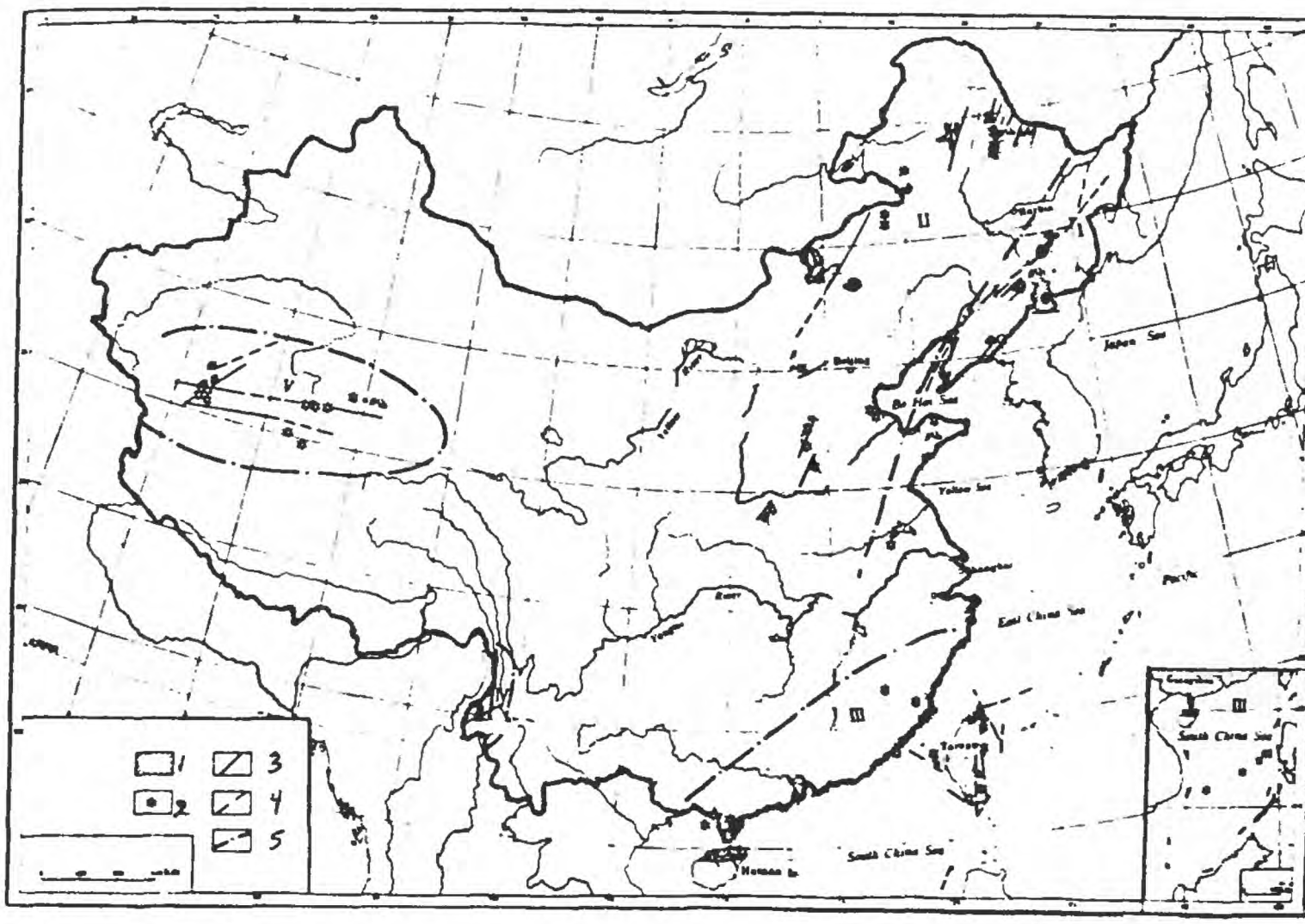

Legend

1 - Quaternary volcanic rocks
2 - Quaternary volcanoes
3 - fracture/fault
4 - inferred fracture
5 - boundary of volcanic belt

Volcanic regions:

I - Changbai Mountains - Longgang Mountains volcanic belt
II - Khingan Mountains - Taihang Mountains volcanic belt
III - Southeastern coastal volcanic belt
IV - Western Yunnan volcanic belt
V - Western Kunlun Mountains - Hoh Xil volcanic belt

Figure 6. Distribution map of Quaternary volcanoes and associated volcanic rocks in China, and their relationship to fractures. (After Zhang Yufang, 1991).

Figure 7. Map showing approximate depth to the Mohorovicic discontinuity in China. The depth contours are in km. (From Meyerhoff and others, 1991).

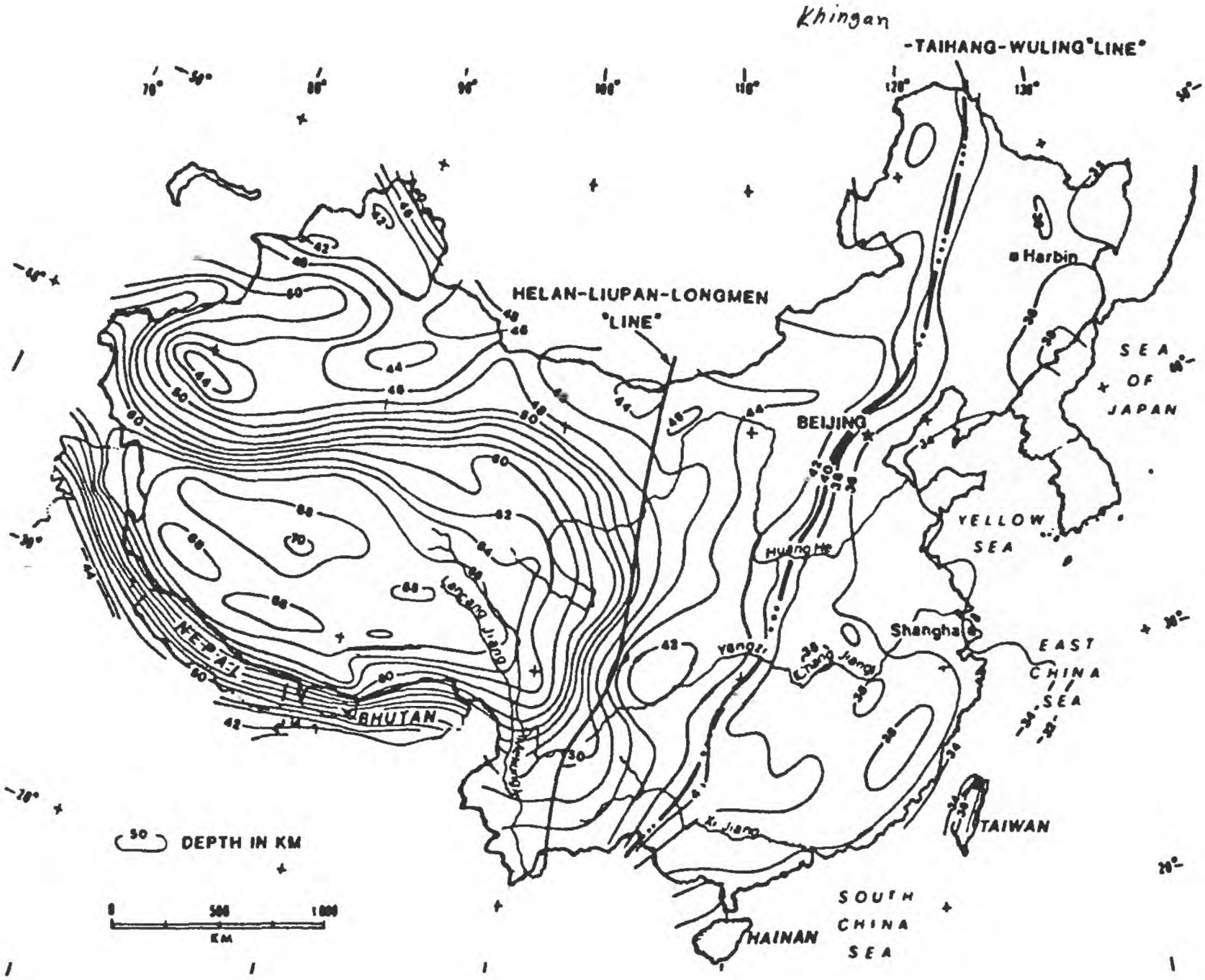

Figure 8. Map showing the location of some of the seismic exploration profiles in China. The numbered boxes are keyed to numbered regions in Table 1. (From Huang and Wang, 1991b).

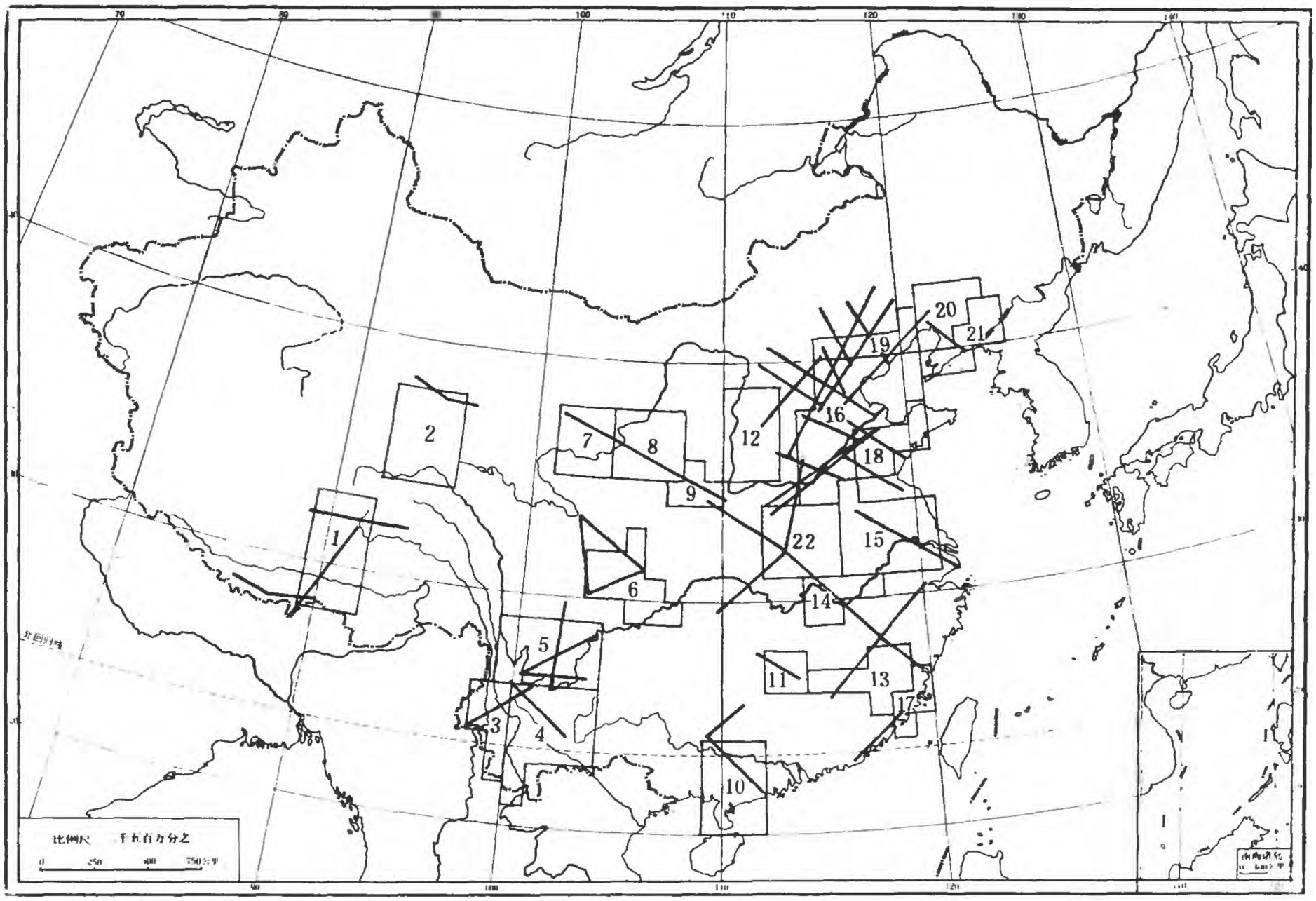

I

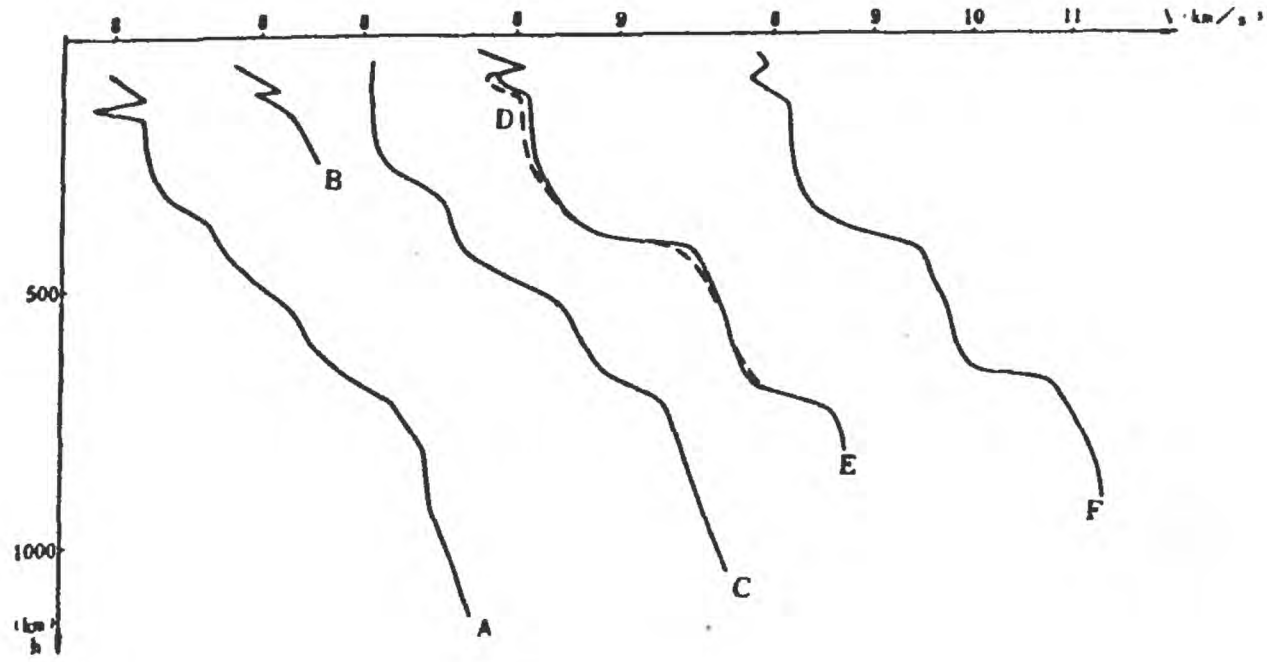

II

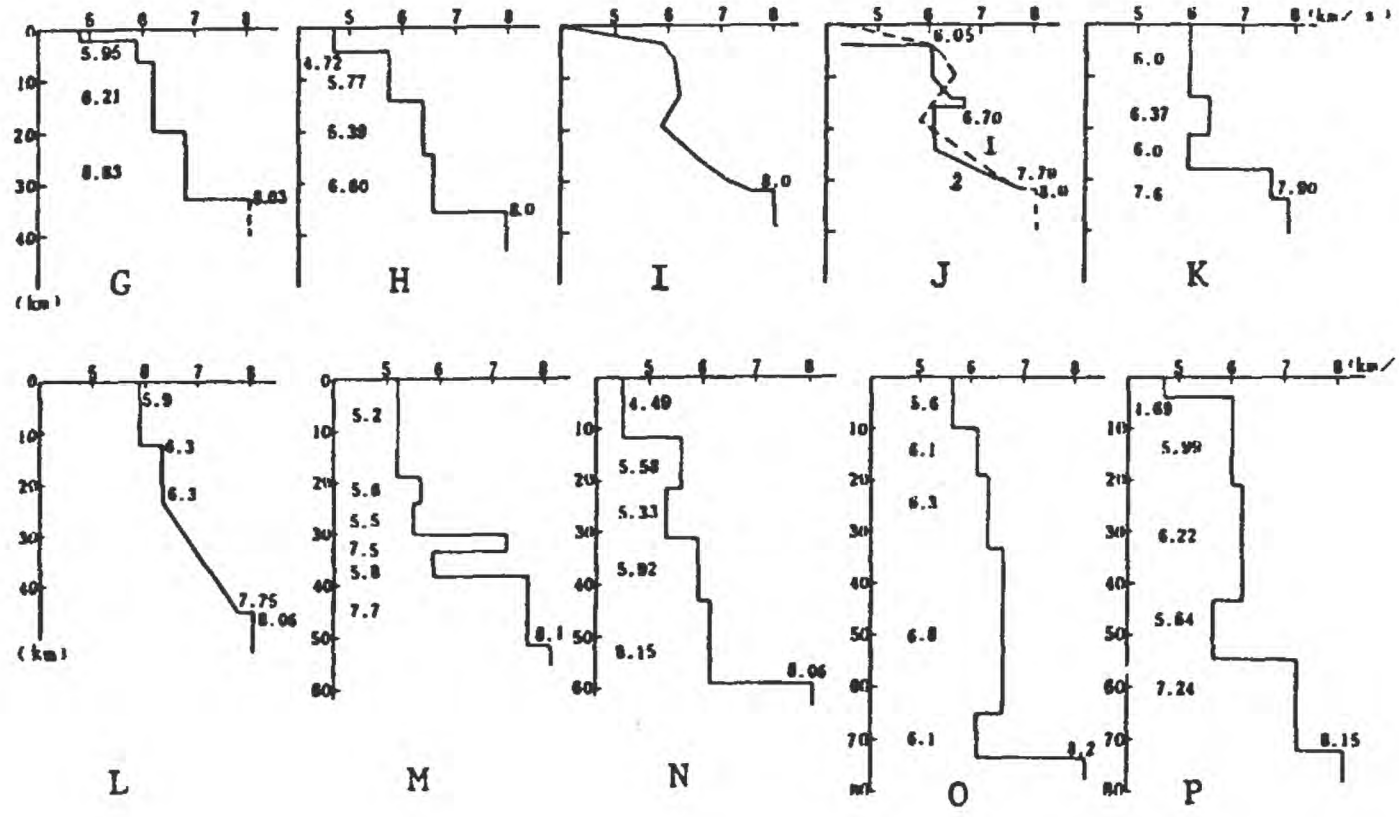

A - Qinhai-Xizang
B - N-S trending belt (between 102^0 to 105^0 E)
C - South China
D - Yellow Sea
E - East China Sea and South China Sea
F - North China
G - Yongping, Jiangxi Province
H - South China
I - southern part of North China
J - northern part of North China
K - Southern part of Liaoning Province
L - Western Yunnan
M - Qaidam basin
N - Tarim basin
O - north of the Himalayas
P - north of Yarlung Zangbo River

Figure 9. I) P-wave velocity models of the lithosphere and upper mantle of various areas of China, to about 1,000 km depth; and II) crustal velocity structures of various parts of China, to 40 - 80 km depth. (After Ma Xingyuan, 1986).

Figure 10. Distribution of seismic events throughout China, utilizing historical data dating to 1200 B.C.; and instrumented data to 1990. The magnitude range of the events displayed is from 3.5 to 9.0. The locations of eight in-country seismic stations are indicated by the solid triangles. (From USGS Global hypocenter database CD-ROM, 1990b).

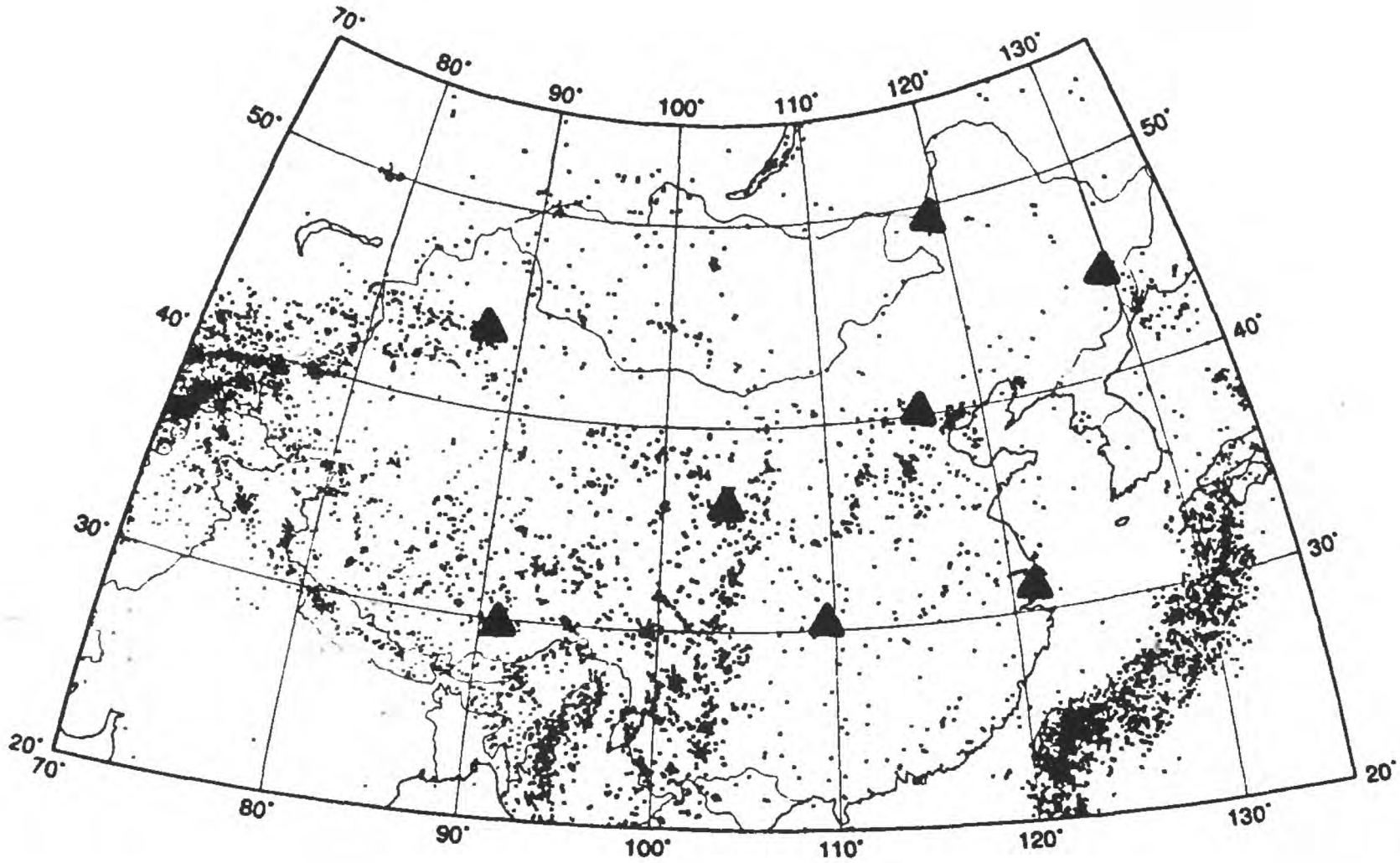

Figure 11. Seismic intensity zoning map of China. The regions characterized by intensity >IX correlate to the areas with a greater density of seismic events, as given on the seismicity map of Figure 10. (From the Compiling Committee of Seismic Zoning Map in China, 1992).

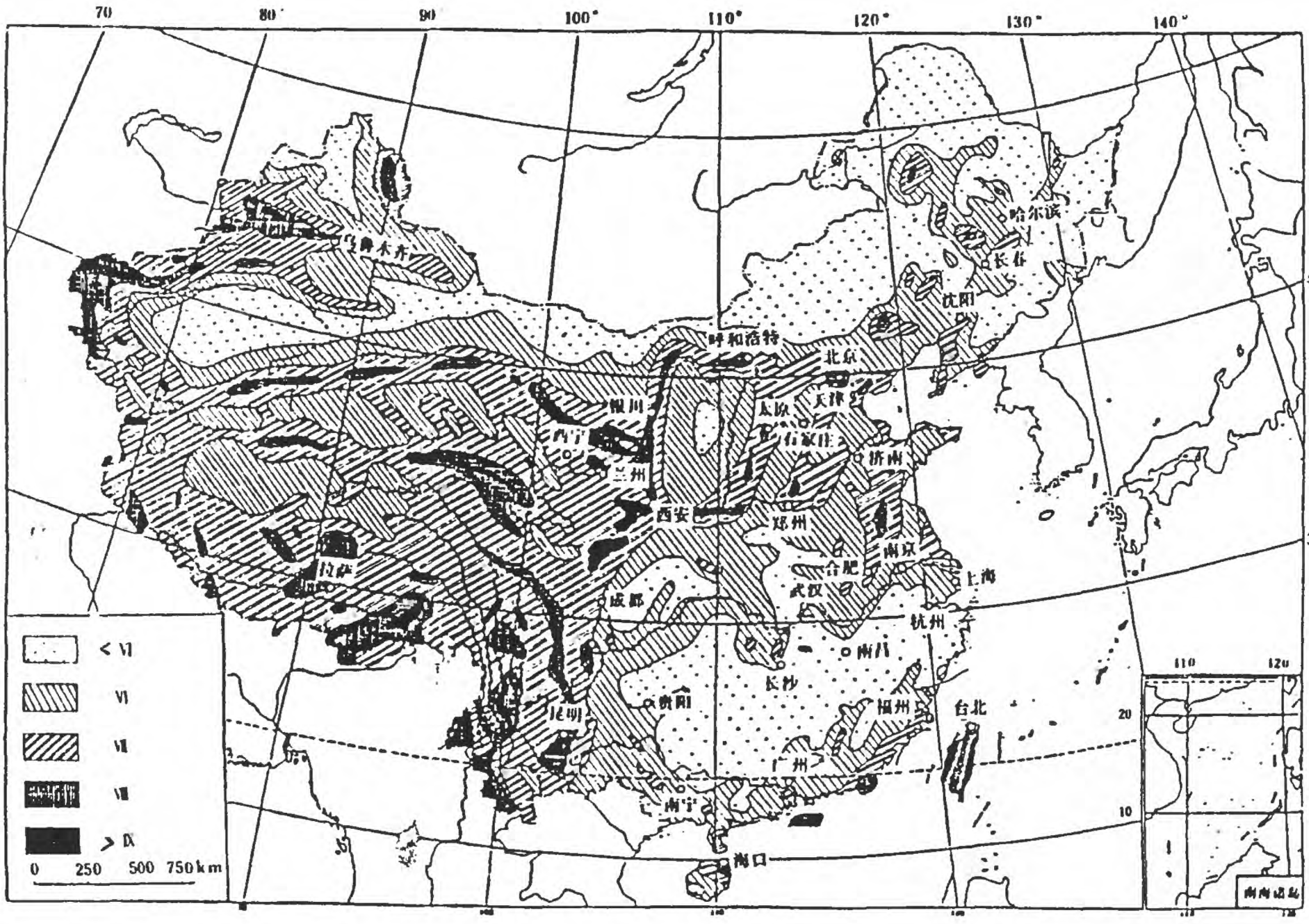

Figure 12. Quality weighted average heat flow for the continental area of China. Average heat flow values are in mW/m^2. (After Huang and Wang, 1991b).

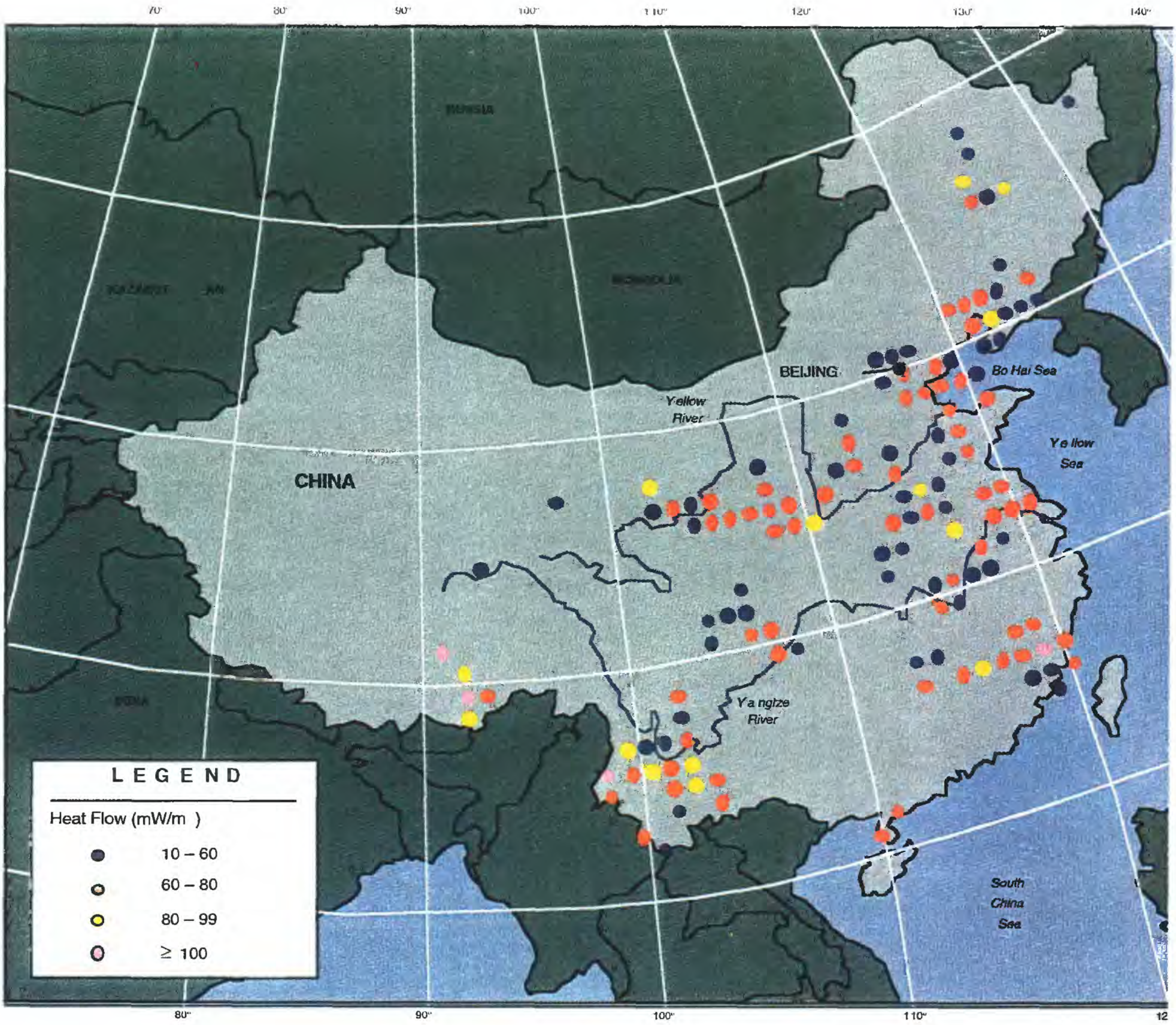

Figure 13. Temperature structure of the crust and upper mantle along the Luyang - Haicheng - Donggou profile. (From Zaoxun Lu and others, 1991).

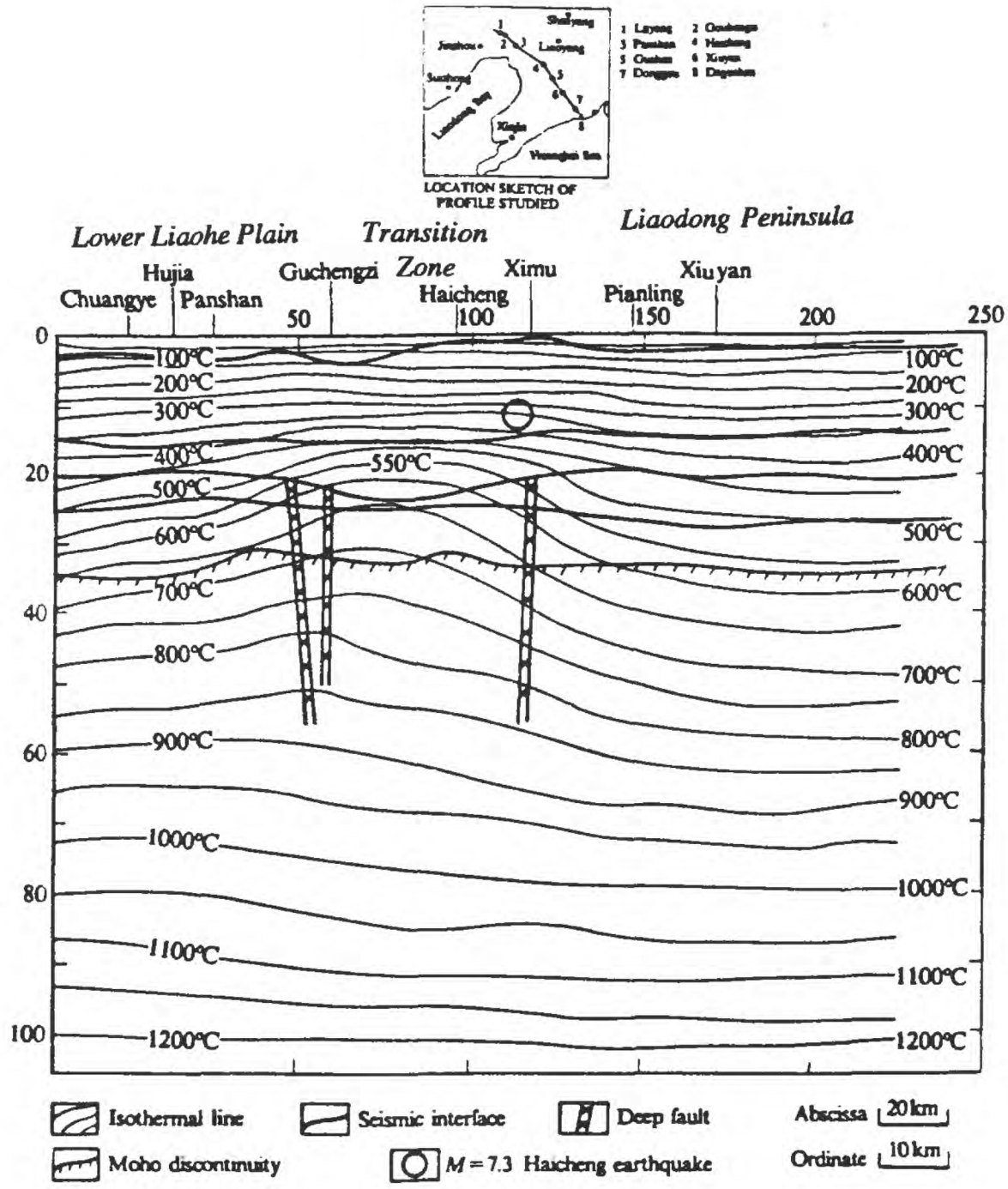

Main deposits and mines; provinces

1. Toksun Xian; Xinjiang
2. Harqin; Nei Monggol
3. Dalian; Liaoning
4. Huai an Xian; Jiangsu
5. Qarhan, Qaidam; Qinghai
6. Nagqu; Xizang
7. Dongyuan; Anhui
8. Zigong/Fushun; Sichuan
9. Qingjiang; Jiangxi
10. Hainan Dao; Guangdong

Figure 14. Location of salt mines and deposits in China. (From Werner, 1988).

Figure 15. Distribution of salt structures in the Qianjiang depression, Jianghan basin, Hubei province. (From Xie Taijun and others, 1988, p. 356).

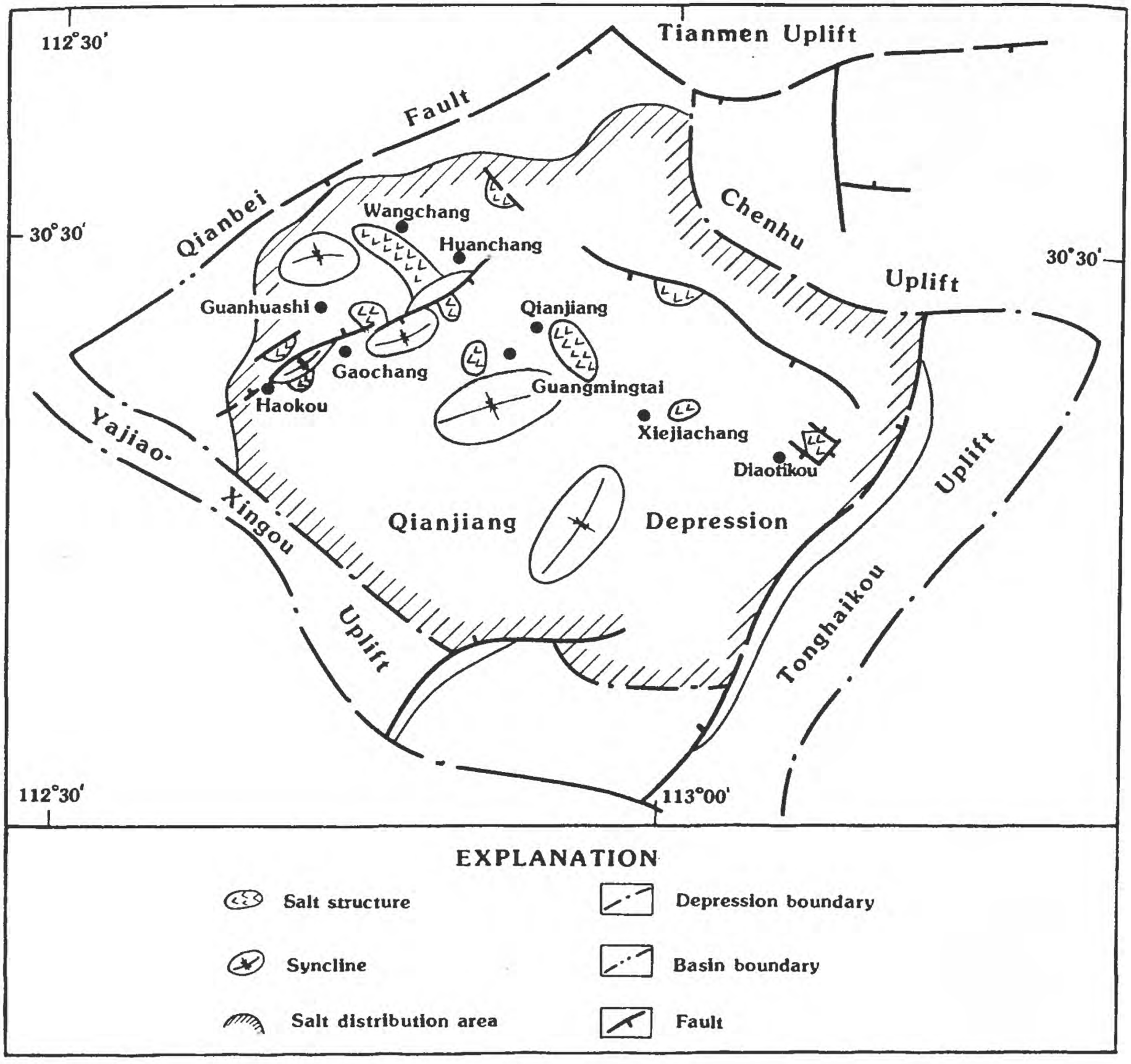

Figure 16. Location of the major known oil and gas fields in the sedimentary basins of China. After Lee and Masters, 1988.

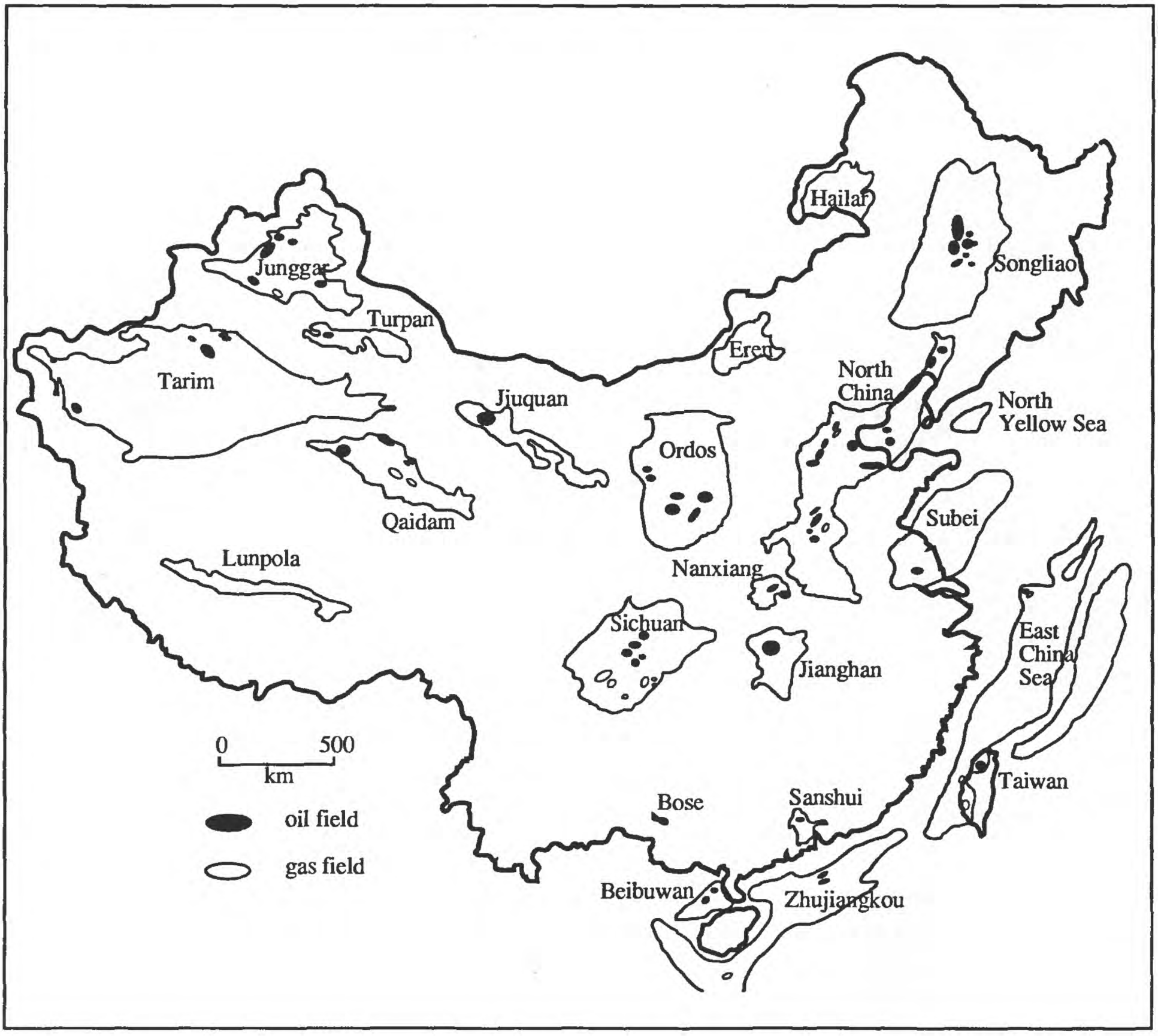

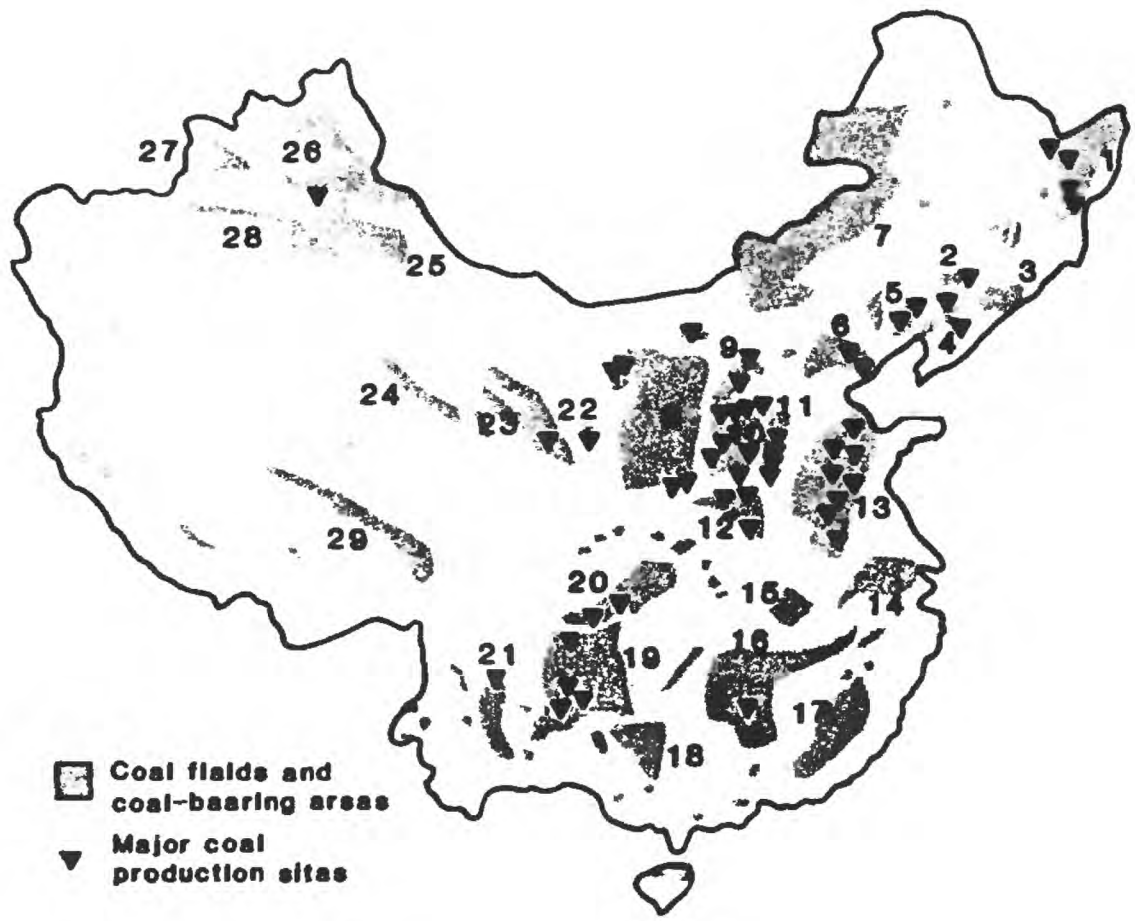

Coal region	Field, province, or area	Coal region	Field, province, or area
1	Sanjiang-Muling area	16	Hunan, Jiangxi, and Guangdong provinces
2	Northern Liaoning	17	Fujian and Guangdong provinces
3	Hun River area	18	Central Guangxi Zhuang Autonomous Region
4	Liao River and Taizi River area	19	Guizhou, Yunnan, and Sichuan provinces
5	Western Liaoning	29	Huayingshan mountain area
6	Beijing-Tangshan area	21	Central Yunnan province
7	Eastern Inner Mongolia Autonomous Region	22	Hexi corridor area
8	Erdousi coal field	23	Datong River area
9	Daning coal field	24	Qaibei area
10	Qinshui coal field	25	Turpan-Hami coal foeld
11	Eastern foot of the Taihangshan mountains	26	Junggar coal field
12	Western Henan province	27	Yili area
13	Jiangsu, Shadong, Henan, and Anhui provinces	28	Northern fringe to Tarim
14	Zhejiang, Jiangsu, and south Anhui area	29	Northern Xizang Autonomous Region
15	Southeastern Hubei province		

Figure 17. Distribution of coal fields and coal-bearing areas in China. (From Dorian and Fridley, 1988).

Figure 18. Map of the distribution of the metallic mineral resources of China. (From Dorian and Fridley, 1988).

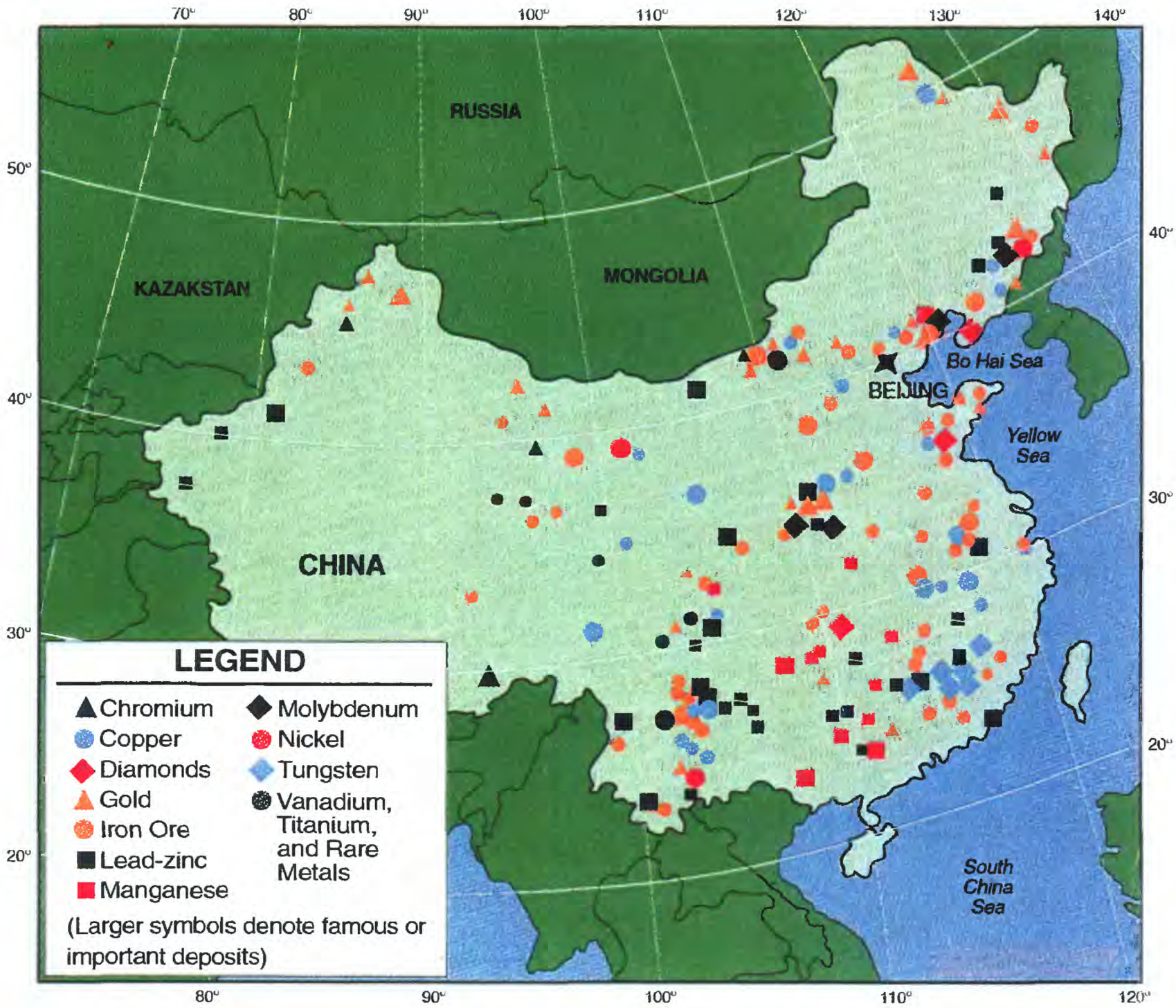

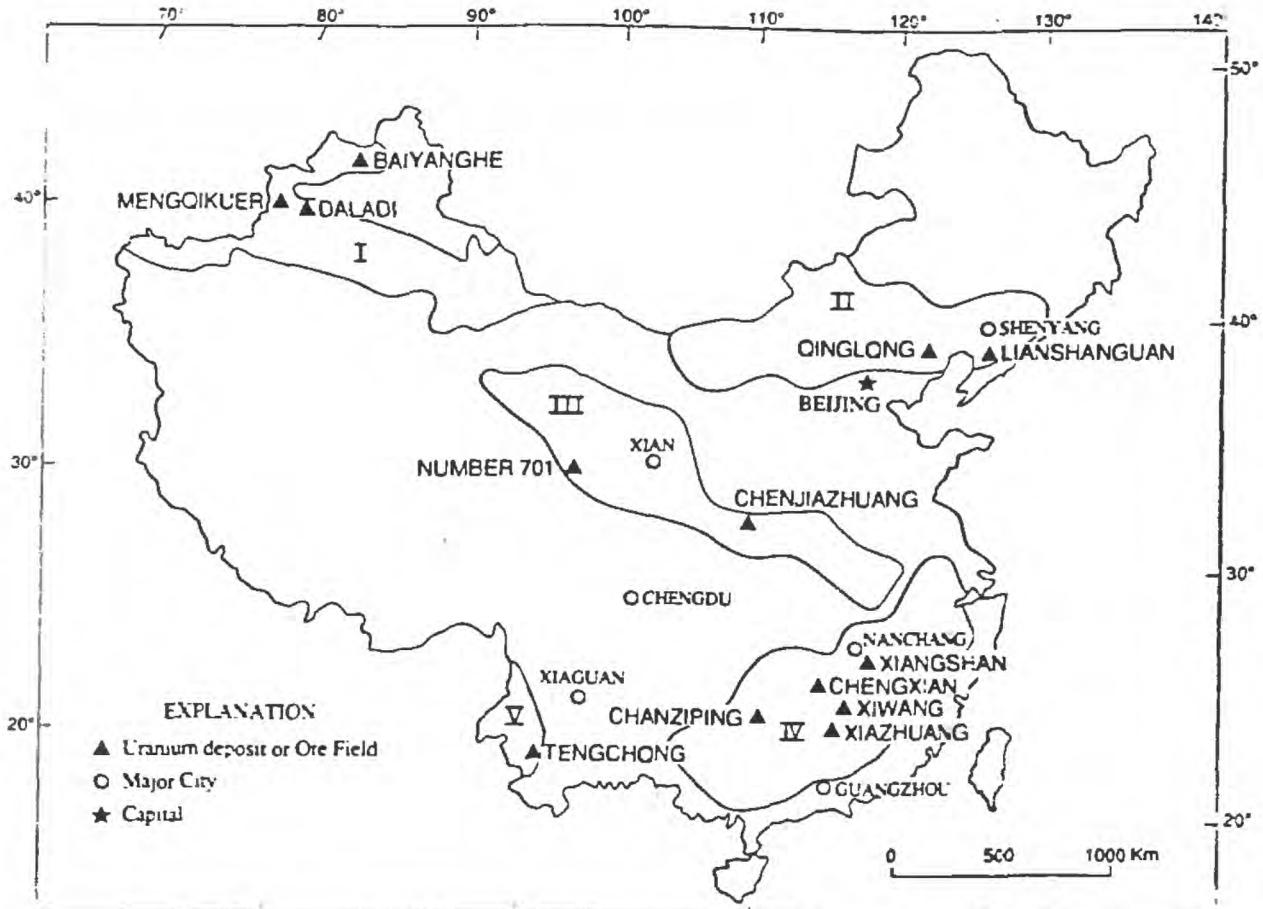

Name of deposit	Political province	Uranium province	Type of deposit
Baiyanghe	Xinjiang	I	volcanic
Chanziping	Guangxi	IV	carbonaceous-siliceous-pelitic
Chengxian	Hunan	IV	carbonaceous-siliceous-pelitic
Chenjiazhuang	Shaanxi	III	intrusive alaskite
Daladi	Xinjiang	I	sandstone
Lianshanguan	Liaoning	II	Precambrian migmatite (metasomatite)
Mengqikuer	Xinjiang	I	sandstone
Number 701	Qinghai	III	carbonaceous-siliceous-pelitic
Qinglong	Hebei	II	volcanic, sandstone
Tengchong	Yunnan	V	sandstone
Xiangshan	Jiangxi	IV	volcanic
Xiazhuang	Guangdong	IV	granite
Xiwang (Number 330)	Guangdong	IV	granite

Uranium provinces:

I - Junggar (Zhungel) - Tianshan
II - Yinshan - Liaohe
III - Qilian - Qinling
IV - South China
V - West Yunnan

Figure 19. Location map of selected uranium deposits and the major uranium provinces in China. (From Finch and others, 1993).

Figure 20. Map of the distribution of carbonate rocks in China. (From Yuan Daoxian, 1992, p. 316).

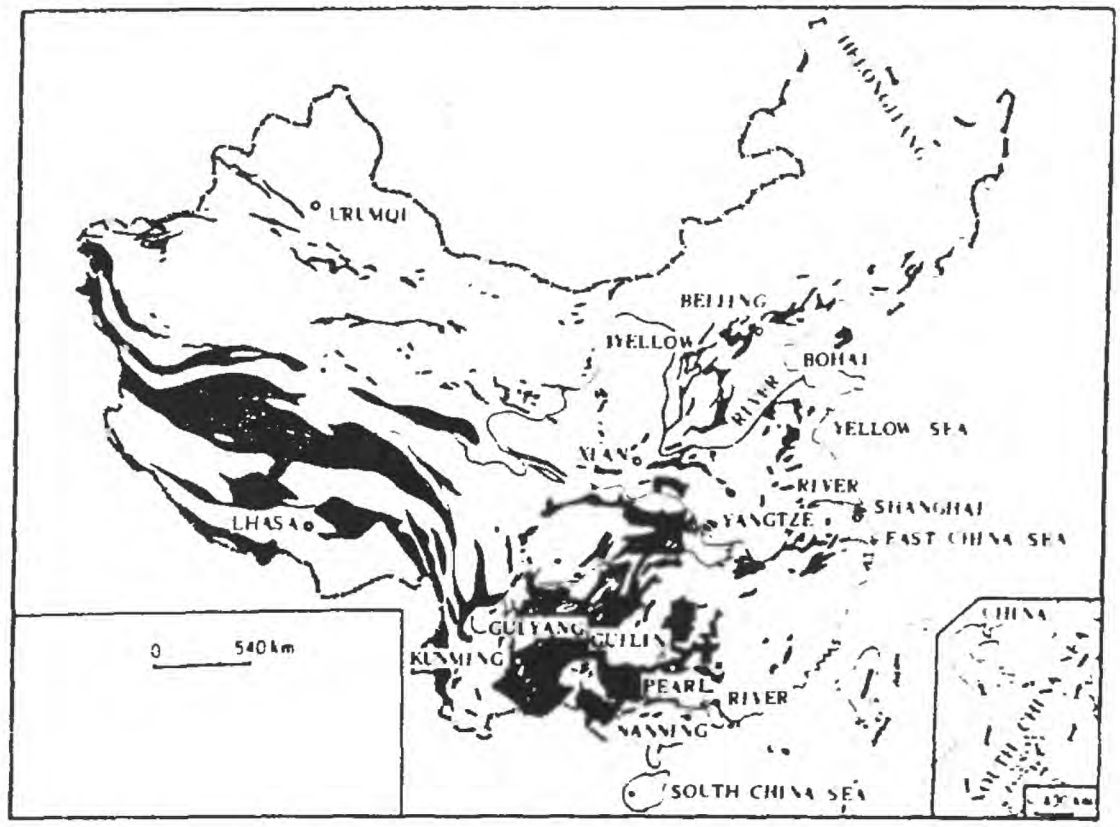

Figure 21. Map of the distribution of loess deposits in China. The location of the Loess Plateau of north-central China is indicated. (From Liu, 1988).

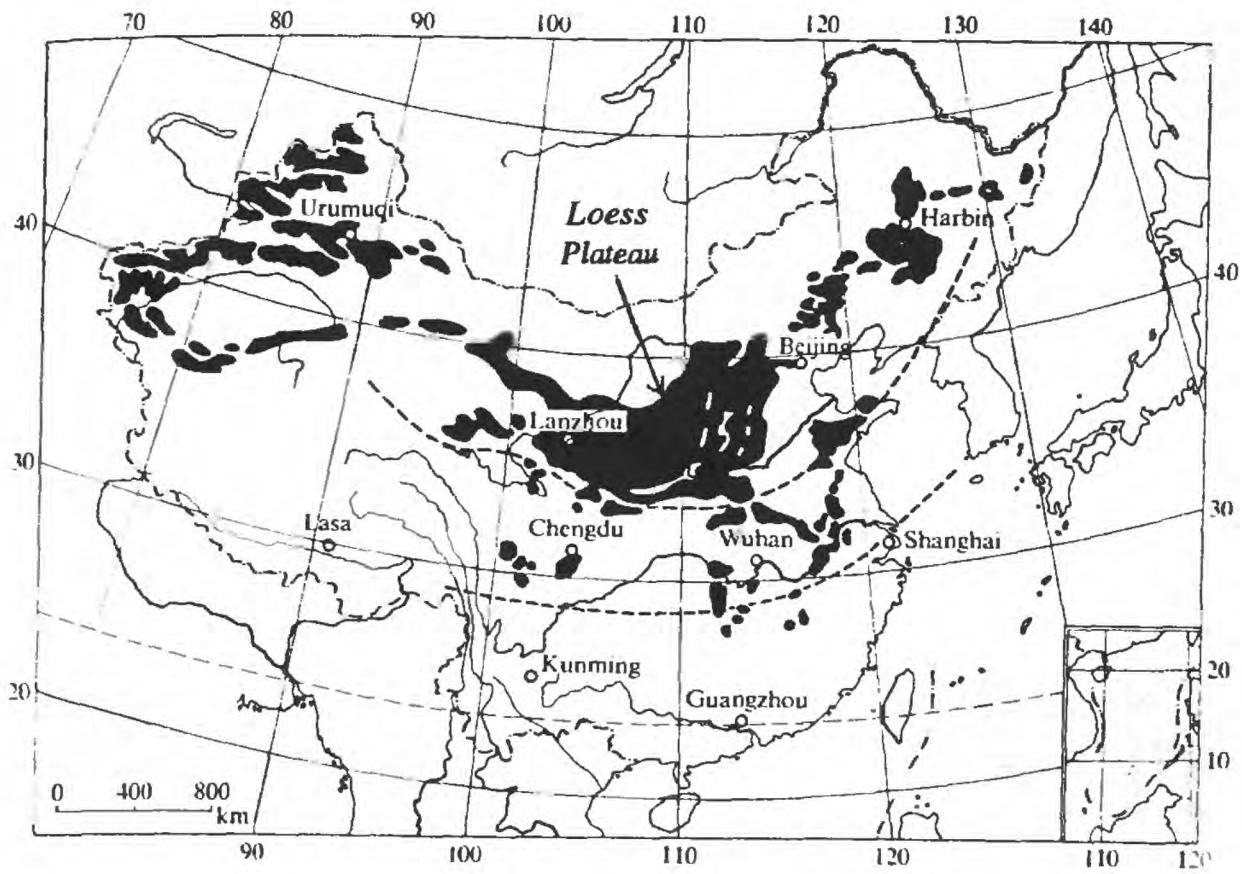

Figure 22. Thickness distribution of the loess in the Loess Plateau, north-central China. (From Derbyshire, 1983, p. 184).

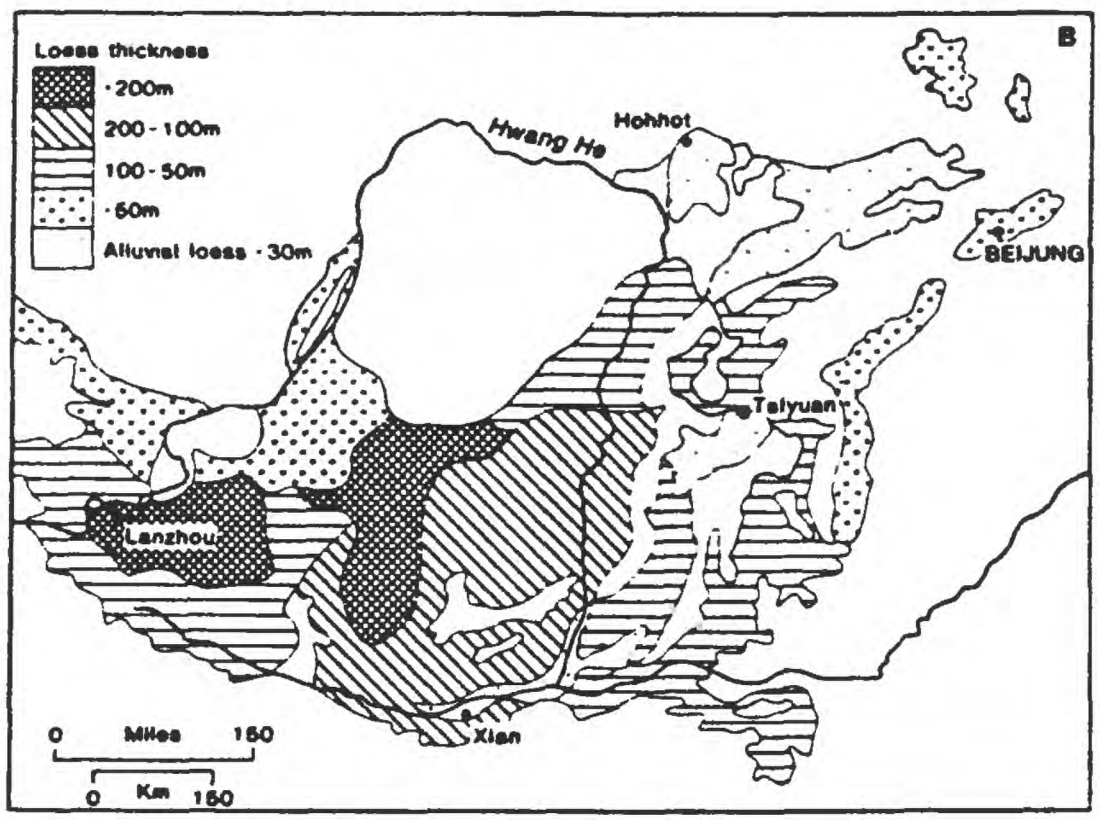

Table 1

Summary of the average Pn velocities, crustal thicknesses, and heat flow data for the 22 boxed areas of Figure 8, in the continental area of China

Box no.	Region	Average Pn velocity (km/sec)	Average crustal thickness (km)	Average heat flow (mW/m^2)
1	Central and Southern Tibet Plateau	8.10	70	99.1
2	Western Qinghai Plateau	8.2	50.9	43.5
3	Western Yunnan	8.06	40	83.1
4	Eastern Yunnan	7.75	42	68.3
5	Panxi Paleorift Zone	7.75	55	67.9
6	Sichuan Basin	8.35	40	58.1
7	Southeastern Qinghai Plateau	7.92	57.2	64.1
8	Southwestern Qinghai Plateau	7.92	43.8	58.9
9	Qinling Fold Zone	7.92	33.2	72.7
10	Zanjian Area	8.09	31.6	68.4
11	Central Hunnan Province	7.86	28.5	45.6
12	Shanxi Plateau	7.85	43	62.9
13	South Jiangxi-North Fujian Fold Zone	8.03	33	79.1
14	Central Yangzhi Platform	8.15	32	57.9
15	Lower Yangzhi Platform	8.0	32	66.1
16	Inner North China Basin	8.15	33	62.4
17	SE Fujian Fold Zone	8.0	29.5	56.5
18	W Shandong Uplift and Jiadong Peninsula	7.85	33	57.3
19	Yanshan Fold Zone	7.85	37	48.0
20	Lower Liaohe Basin	7.64	32	64.4
21	Liaodong Peninsula	7.66	34	52.6
22	Central China Basin	8.03	34	55.5

From Huang and Wang, 1991b

Table 2
Compilation of known salt ocurrences In China

Province	Basin or Area	Rock Type	Structure	Age	Depth (m)	Thickness (m)
Sichuan	Zegong, Sichuan basin	halite anhydrite gypsum	dome	Triassic	840	8 max.
Hubei	Jianghan basin	salt	domes anticlines	Cretaceous to Paleogene		1800 max (1265 in Qianjiang)
Liaoning Hebei Henan	North China basins	salt gypsum	dome-like structure	Tertiary	2000 - 5000	600 - 800
Qinghai	Qaidam basin	salt gypsum		Neogene		
Xinjiang	Turpan basin	anhydrite halite		Neogene		
Xinjiang	Tarim basin	salt				600
Yunnan	Mekong foldbelt	salt		Jurassic		
Ningxia	Ordos basin	salt gypsum				>100 cumulative